Progress in Oceanography 240 (2026) 103601

Contents lists available at ScienceDirect

Progress in Oceanography

journal homepage: www.elsevier.com/locate/pocean

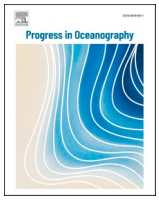

Sub-Antarctic fjord circulation and associated icefish larval retention in a changing climate

Joanna Zanker [a,b,*], Emma F. Young [a], Paul Brickle [c,d], Ivan Haigh [e]

[a] British Antarctic Survey, UK
[b] Northumbria University, UK
[c] South Atlantic Environmental Research Institute, FI, UK
[d] School of Biological Sciences (Zoology), University of Aberdeen, Tillydrone Avenue, Aberdeen, Scotland AB24 2TZ, UK
[e] Ocean and Earth Science, National Oceanography Centre, University of Southampton, Southampton, UK

ARTICLE INFO

Keywords:
South Georgia
Fjord
Oceanography
Mackerel icefish
Lagrangian modelling

ABSTRACT

Climate change is impacting high-latitude fjord circulation with consequences for the transport of marine biota essential for supporting local ecosystems. Currently, little is understood about oceanographic variability in sub-Antarctic island fjords such as Cumberland Bay, the largest fjord on the island of South Georgia in the Southern Ocean. Cumberland Bay is split into two arms, West Bay and East Bay, and is a key spawning site for the ecologically and commercially important mackerel icefish. Through the use of a high-resolution three-dimensional hydrodynamic model, the seasonal cycle in Cumberland Bay is found to be driven by a combination of boundary forcing influencing shelf exchange and deep inflow, atmospheric forcing influencing near surface temperatures and flows and freshwater forcing via subglacial discharge driving upwelling and strong outflow. There is a complex three-dimensional flow structure with a high degree of variability on short timescales due to wind forcing. Using model flow fields to drive an individual-based model parameterised for mackerel icefish larvae spawned in Cumberland Bay, we identify West Bay as a key retention zone. Successful retention of mackerel icefish larvae is found to be sensitive to complex circulation patterns driven by winds, freshwater and fjord-shelf exchanges and to changes in physical processes linked to climate change such as meltwater runoff and föhn wind events. This study highlights the importance of oceanographic variability in influencing ecological processes in fjords in our changing climate.

1. Introduction

A fjord is a long, deep and narrow semi-enclosed coastal inlet, formed through glacial erosion, often containing one or more submarine sills (Farmer and Freeland, 1983; Inall and Gillibrand, 2010). High-latitude fjords may be associated with seasonal sea ice, and in most cases, have a glacier terminating at the fjord head. Predominantly, these fjords are located in the Arctic, such as Greenland and Svalbard, but they are also found on sub-Antarctic islands in the Southern Ocean and on the Antarctic Peninsula (Cook et al., 2010; Griffith and Anderson, 1989). Fjords generally consist of a relatively fresh surface layer, intermediate layers, and a deep, high salinity layer (Cottier et al., 2010; Skarðhamar and Svendsen, 2010). The layers are impacted by variability in water masses, circulation and exchange on the adjacent shelf, and the presence and depth of a sill. There is usually a strong seasonality, driven by freshwater inputs and air-sea interactions, with a high degree of stratification in the summer and relatively weaker stratification in winter.

The importance of circulation dynamics within high-latitude fjords can be separated into a few key aspects. There is evidence that fjord circulation directly governs the stability of tidewater glaciers at the ice-ocean interface, as warm water circulating from the open ocean into the fjord induces melt at the submarine ice face (Mortensen et al., 2014; Straneo et al., 2010). Frontal ablation of tidewater glaciers directly contributes to sea-level rise (Benn et al., 2017; Straneo et al., 2010), and studies have shown that ocean warming is accelerating mass loss from tidewater glaciers (Christoffersen et al., 2011; Mortensen et al., 2011; Straneo et al., 2010). Fjords indent the coastline and may provide sheltered zones for the retention and growth of the early life stages of marine organisms (Asplin et al., 1999; Young et al., 2011). Biological productivity is extremely high in fjords, with the marine ecosystem

* Corresponding author at: Room 221A, Ellison Building, Northumbria University, Newcastle upon Tyne, NE1 8ST, UK.
E-mail address: jo.zanker@northumbria.ac.uk (J. Zanker).

https://doi.org/10.1016/j.pocean.2025.103601
Received 7 February 2025; Received in revised form 20 October 2025; Accepted 22 October 2025
Available online 27 October 2025

supporting large colonies of higher predators such as sea birds and marine mammals (Ward, 1989; Węsławski et al., 2000). Often, fjords are spawning grounds for fish which may play a key role within the ecosystem and have commercial importance (Everson et al., 2001; Myksvoll et al., 2011; Synnes et al., 2021). The fjord circulation and shelf exchange control the transport and retention of fish larvae, an understanding of which is vital for the management of local fisheries (Everson, 1992).

Following previous work, it is helpful to characterise fjord circulation into four main modes (Mortensen et al., 2011). Firstly, estuarine circulation is driven by fresh meltwater input into the surface layer at the head of the fjord. This causes an outflow of relatively fresh water,

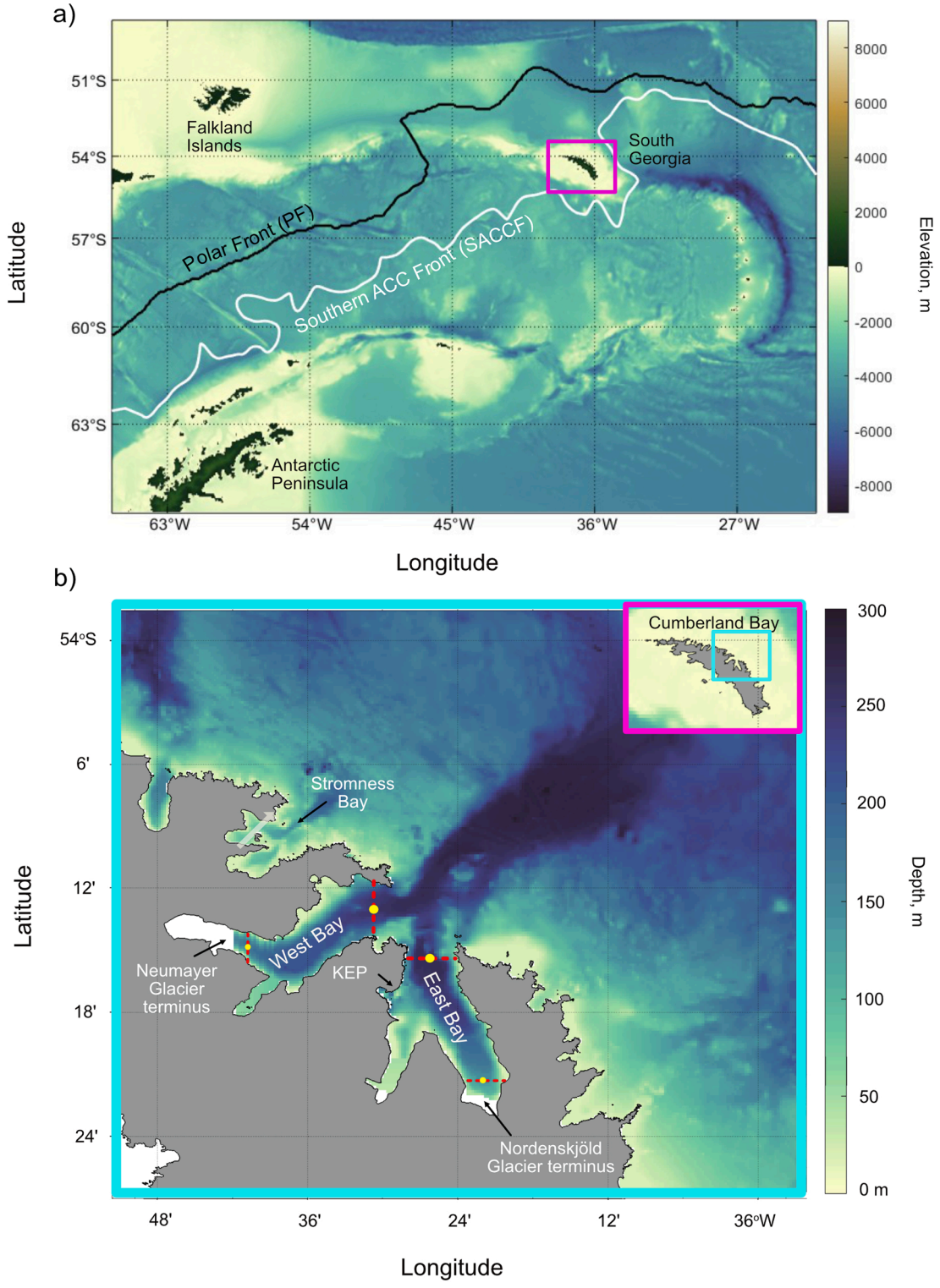

Fig. 1. (a) A map of South Georgia's position in the Southern Ocean (pink box) with positions of the Polar Front and the Southern ACC Front labelled; (b) the model domain, detailing the bathymetry of Cumberland Bay. Red dash lines show the position on the cross-sections and yellow dots show the locations of single point temperatures and salinities used in model analysis.

setting up a salinity gradient causing entrainment of water into the surface layer from below (Talley et al., 2011). Secondly, buoyancy-driven circulation is driven by meltwater runoff at the grounding line emerging as a buoyant plume and rising in contact with the glacier face. This freshwater plume entrains relatively warm and dense water, resulting in a slow but thick inflow at depth, and a thin and fast outflow of relatively fresh water in the surface layer or where the plume reaches neutral buoyancy at depth (Sciascia et al., 2013). Thirdly, dense coastal inflow into the deeper parts of the fjord is driven by density differences between the coastal current system and water masses within the fjord (Arneborg et al., 2004). The inflowing dense coastal currents displace the bottom layer within the fjord and create a compensating outflow. Finally, intermediary circulation is a result of fluctuations in shelf water density driving exchange at the fjord mouth (Jackson et al., 2018).

These four characteristic modes of fjord circulation can be modified by a multitude of internal and external processes, which can additionally drive further modes of circulation. Wind stress, tides, shelf-fjord exchange, and freshwater input are the main mechanisms forcing the extent of vertical and horizontal circulation, as well as modifying, mixing, and exchanging water masses (Cottier et al., 2010; Inall and Gillibrand, 2010). Local winds have a significant impact on surface velocities and are commonly katabatic in fjords, steered along-axis by local topography (Inall and Gillibrand, 2010; Spall et al., 2017). Winds steered towards the fjord head will tend to drive freshwater up-fjord, inducing a compensating subsurface outflow, while winds towards the fjord mouth will enhance estuarine circulation or buoyancy-driven outflow, driving subsurface inflow (Cottier et al., 2010; Inall and Gillibrand, 2010). Due to the Coriolis Effect, net wind-driven transport of water is to the left (right) of the wind direction in the southern hemisphere (northern hemisphere), leading to associated coastal up/down welling in the shelf region outside the fjord. This results in changes in horizontal density gradients which impacts fjord-shelf exchange.

In our changing climate, increased melting of glaciers within fjords due to ocean and atmospheric warming introduces higher volumes of fresh meltwater, which alters stratification and the circulation regime (Slater and Straneo, 2022; Straneo and Cenedese, 2015). Additionally, the retreat of glaciers leads to the exposure of the fjord basin, potentially revealing key topographic features such as sills, and deep inner basins. These new areas of fjords and changes in oceanography could have strong implications for biological activity and ecosystem dynamics (Bosson et al., 2023), for example, by providing new habitat with preferential growth conditions, or by increasing the retention of early life stages of organisms (Wesławski et al., 2011). Changing wind conditions may also have a strong impact on ecological processes, in particular the transport of planktonic organisms and nutrients in the surface layers of the fjord (Asplin et al., 1999).

These types of changes may be particularly important in the heavily glaciated sub-Antarctic island of South Georgia, which hosts a rich ecosystem of marine mammals, penguins, and flying seabirds, and is a feeding ground for whales (Barlow et al., 2002; Calderan et al., 2023; Clarke et al., 2012). The island sits in the path of the Antarctic Circumpolar Current (ACC) (Fig. 1a). The Southern ACC Front, which loops anticyclonically around the island, plays a major role in transporting krill, a key prey item for higher predators, to the island (Trathan et al., 2003). There has been an overall negative mass balance for the island's glaciers over the past century, in line with global glacier mass loss under warming temperatures (Farías-Barahona et al., 2020; Rounce et al., 2023; Zemp et al., 2019). The resulting increase in glacial meltwater runoff may directly influence the ecosystem by driving variability in fjord circulation and transporting zooplankton and nutrients that are essential for primary production (Arimitsu et al., 2016; Robinson et al., 2016).

The island is located in a belt of strong westerly winds, with the central southeast-northwest mountain range along the spine of the island orientated as a barrier to the prevailing wind, giving rise to warm, dry, downslope winds descending on the lee-side of the mountain range, known as föhn winds (Bannister and King, 2020). Föhn wind events are experienced ~ 30 % of the time on the northeast coast and are generally longer and more intense in the austral summer (Bannister and King, 2020). They are a significant feature of the local climate and appear to be correlated with large-scale atmospheric circulation. Analysis of climate records from the island for the periods 1905 – 1982 and 2001 – present has revealed a temperature rise of 0.13∘C per decade and a long-term increase in precipitation of 45.1 mm per decade (Thomas et al., 2018). The warm extremes recorded were related to stronger westerly winds and föhn wind events.

Cumberland Bay is the largest fjord on the island, situated on the northeast coast and split into two arms, West Bay (WB), where Neumayer Glacier terminates, and East Bay (EB) where Nordenskjöld Glacier terminates (Fig. 1b). These glaciers exhibit asymmetrical behaviour, having retreated at markedly different rates, representative of the island's glaciers as a whole. The drivers of the asymmetric retreat within Cumberland Bay were investigated by Zanker et al., (2024), finding that the rapid retreat of Neumayer Glacier in WB may be due to the presence of a shallow inner sill interacting with buoyancy-driven outflow. There may also be differential melting of these glaciers driven by ocean and atmospheric processes, such as föhn winds (Bannister and King, 2020).

Cumberland Bay is an important spawning ground for fish, including mackerel icefish (*Champsocephalus gunnari*) which are a key component of the local food web and the target of a commercial fishery (Everson et al., 2001; Frolkina, 2002). *C. gunnari* stock size in South Georgia is highly variable, with an overall decline in recent years (South Georgia and the South Sandwich Islands Mackerel Icefish Fishery Management Plan 2019–2020), which may be due in part to variability in the retention and recruitment of larvae, which is influenced by oceanographic variability (Young et al., 2012). The South Georgia and South Sandwich Islands Marine Protected Area (SGSSI-MPA), set up in 2012, is one of the world's largest MPAs, and protects against overfishing and exploitation (Trathan et al., 2014). In addition to the MPA, the government of SGGSI has its own fisheries legislations with stock assessments reported to the Commission for the Conservation of Antarctic Marine Living Resources (CCAMLR), which sets quotas and regulations on the few legal fisheries operating in the area. One such fishery exists for *C gunnari*.

Champsocephalus gunnari is a bentho-pelagic species found predominantly around islands of the Scotia Arc, Kerguelan, Heard, and Bouvet islands in the Southern Ocean, and the southernmost South Atlantic Ocean (Everson, 2003). There is still relatively little known about the spawning habits of *C. gunnari.* Based on current knowledge, peak spawning time in South Georgia is from March to May, though there is evidence of spawning outside of this time (Belchier and Lawson, 2013). Spawning typically takes place within fjords and deeper, inshore parts of the shelf at depths between 100–300 m (Frolkina, 2002; Kock, 1989; Parkes et al., 2000). The eggs, around 3 – 4 mm in diameter, are assumed to be laid on the bottom (Everson et al., 2001; Kock and Everson, 1997), and the potential fecundity for mackerel icefish is between ~ 1200 to 31000 eggs per fish each season (Kock and Everson 1997; Everson, 2003). Incubation is roughly three months, and hatching occurs as early as June, but predominantly between August and October (Frolkina et al., 1998; Everson et al., 2001; Kock and Everson, 1997). *C. gunnari* larvae are concentrated in coastal regions between 3.5 and 19 km offshore, predominantly within bays (Everson et al., 2001; Frolkina, 2002; Kock and Everson, 1997). Larval concentrations within Cumberland Bay have been found to be an order of magnitude higher than in adjacent coastal waters (Everson, 2003; Everson et al., 2001). In Cumberland Bay, year-round sampling found early larvae present from July to November most abundantly but lower numbers are present as early as April (Belchier and Lawson, 2013; Everson et al., 2001). The time taken for larvae to develop from hatching to juvenile stage has been estimated to be between 3 and 5 months (Duhamel et al., 1995), with those hatched later in the year potentially able to catch up, in terms of development, with those hatched earlier (North, 2001). The larvae are found to be most

abundant in the upper 100 m of the water column and feed mainly on copepods and copepod eggs (North and Murray, 1992).

The management of icefish fisheries requires ecosystem-based decisions (Everson, 1992; Fogarty, 2014; Howell et al., 2021; Main et al., 2009). Understanding the ecological relationship between the harvested population and the rest of the ecosystem will better allow for effective conservation measures. Knowledge of spawning locations, growth, mortality, retention, recruitment, and predator–prey interactions provides information to underpin and improve the quality of management (Main et al., 2009). The protection of spawning grounds and retention zones on the shelf and fjords of South Georgia is an important conservation measure, as larval dispersal plays a key role in determining populations and adult stock maintenance (Young et al., 2018).

The retention of fish larvae spawning in fjords is controlled by fjord and shelf circulation, which entraps the larvae (Landaeta et al., 2012; Meerhoff et al., 2014). Wind mixing, turbidity caused by ice melting, and meltwater runoff can disturb density gradients, generating currents, which can transport larvae and alter food availability (Landaeta et al., 2012; Meerhoff et al., 2014; Myksvoll, 2012). Coastal and bottom topography in and around fjords can cause reduced flow and create retention zones (Cowen and Sponaugle, 2009). Temperature can play a key role in the life cycle of fish species such as *C. gunnari* including spawning phenology and rates of egg and larval development (Hinrichsen et al., 2011; Hsieh et al., 2009; Lett et al., 2010). A detailed understanding of fjord circulation and stratification alongside behaviour, such as spawning sites, vertical migration, and growth time-scales is required to predict where and when fish larvae may be transported and retained within a fjord such as Cumberland Bay. Successful management of the fish population requires this knowledge of early-life dispersal, connectivity pathways, and key retention zones, alongside knowledge of trophic interactions (Hinrichsen et al., 2011; Lett et al., 2010; Young et al., 2018).

An understanding of physical processes influencing fjord circulation can be gained through process test studies. With the use of a three-dimensional hydrodynamic ocean model, processes such as freshwater inputs and wind forcing can be turned on and off, which enables analysis of their impact on the circulation and how such circulation may be affected by a changing climate. For the study of how physical processes impact ecology, individual-based models (IBMs) have been used by coupling biological processes of fish species with spatial and temporal physical dynamics (Hinrichsen et al., 2011; Young et al., 2014). These models can help identify factors influencing reproductive success driven by ocean and atmospheric variability and identify essential habitats for early life stages (Hinrichsen et al., 2011). In particular, IBMs can aid the understanding of the effects of climate change on larval dispersal, including changes in circulation and water temperature driven by local and large-scale perturbations (Lett et al., 2010).

The first aim of this study is to identify the key physical drivers of oceanographic variability in Cumberland Bay, South Georgia, using a numerical fjord circulation model. The second aim is to investigate the implications of such drivers for the transport and retention of the larvae of the commercially and ecologically important *C. gunnari* in a changing climate. The paper is structured as follows. Section 2 details the methods used for the hydrodynamic model process testing and the IBM. Section 3 details the results from the process tests and IBM. Section 4 discusses the implications of the results on the temporal and spatial variability in circulation and the influence of physical processes linked to climate change icefish larvae transport and retention in the fjord. Model caveats are also discussed in Section 4 before a summary and conclusions in Section 5.

2. Methods

Observational data for the oceanography of Cumberland Bay are limited. Conductivity, Temperature and Depth (CTD) casts have been used to help validate a 3D hydrodynamic model of the circulation regime in Cumberland Bay and the adjacent shelf, described in detail in Zanker et al., (2024). A brief summary of the model is provided here. The model has been developed in the NEMO4 (Nucleus for European Modelling of the Ocean v4) (Madec & the NEMO Team, 2019) framework and has a horizontal resolution of ~ 200 m (varying with latitude) with variable vertical resolution decreasing from 1 m at the surface to ~ 30 m at depth.

The model bathymetry was derived from a bathymetric data set compiled by (Hogg et al., 2016) by averaging the 100 m resolution data onto the ~200 m grid (Fig. 1b). The model is forced at the open boundaries with tides from a global tidal model (TPXO9.2; Egbert and Erofeeva, 2002) using eight tidal constituents (Q1, O1, P1, K1, N2, M2, S2, K2) and with 3D flows, sea surface height, temperature, and salinity derived from a regional South Georgia model (Young et al., 2016). Surface boundary forcing is derived from the ERA5 reanalysis data set with 31 km horizontal grid resolution (Hersbach et al., 2020).

The meltwater runoff contributions via surface run-off and subglacial outflow in the domain are taken from a theoretical climatological annual cycle calculated from historical precipitation data, glacier basin size, and positive degree days (Young et al., 2011). For the two large marine-terminating glaciers in Cumberland Bay, the theoretical meltwater cycle is split into 10 % surface runoff and 90 % subglacial discharge based on the assumption that a majority of surface meltwater would enter a subglacial drainage system at the bed through crevasses and moulins (Chu, 2014). Zanker et al. (2024) developed a parameterisation for the buoyant plume arising from subglacial discharge which captured the effect of increased buoyancy-driven outflow and upwelling of deep waters (following similar frameworks implement within MITgcm and ROMS by Cowton et al. (2015) and Oliver et al. (2020), respectively). A brief description is provided here. The parameterisation utilises an off-line plume model based on Slater et al. (2017). The plume model requires inputs of subglacial discharge (90 % of the climatological meltwater cycle), and ambient temperature (^{o}C) and salinity which is gained from a 10-year (2001 – 2010) model run with no terrestrial meltwater forcing. The output from this plume model is a daily buoyancy-driven volume per second ($Q_p m^3 s^{-1}$) of 'modified meltwater' (Fig. 2a), resulting from a plume reaching neutral buoyancy after entraining ambient ocean water at depth. The plume model output for Neumayer Glacier in WB and Nordenskjöld Glacier in EB, are then introduced into the surface layer of the ocean model at a grid cell adjacent to the respective glacier down to the depth of neutral buoyancy for the years 2001 – 2010 (Fig. 2). The remaining 10 % of the climatological meltwater cycle is inserted into an adjacent grid cell to simulate surface runoff generating from supraglacial streams.

Although there is no interannual variability in the theoretical climatological annual cycle, a small amount of interannual variability is captured via the ambient ocean conditions which are forced by the open and surface boundaries (Fig. 2). The combination of surface freshwater and modified meltwater is hereafter referred to as 'meltwater forcing'. The volume flux of the modified meltwater forcing (peaking > 2000 $m^3 s^{-1}$, Fig. 2a) is much greater than the meltwater flux inserted as subglacial discharge (peaking at ~ 35 $m^3 s^{-1}$, Zanker et al., 2024, Figure 3a)), due to entrainment. Contained in the total meltwater forcing is also the surface freshwater runoff from the few small land terminating glaciers in Cumberland Bay. Full details of this parameterisation can be found in Zanker et al. (2024) and in the appendix below.

The model lacks ice-ocean–atmosphere coupling, and thus the timing and volume of the glacier meltwater may be inaccurate. There is no sea ice in the model as Cumberland Bay only sees intermittent seasonal formation of pancake ice, but the influence of melting from ice mélange in general is not captured. The flows generated by entrainment of ocean waters into the vertically rising plume are not included in this NEMO4 parameterization as it is not currently possible to remove ocean water. Therefore, the ocean model does not capture the extent of a thick, but slow inflow below the plume's neutral buoyancy (Cowton et al., 2015;

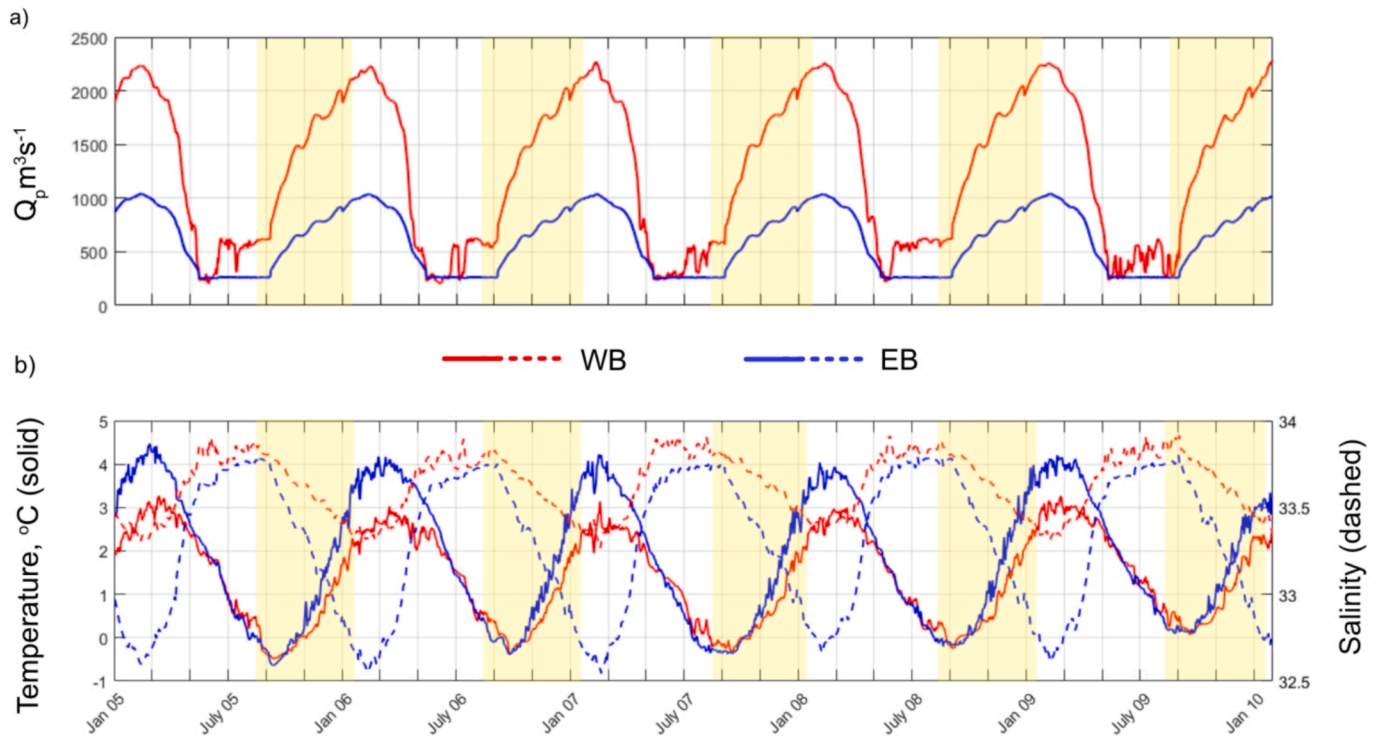

Fig. 2. The properties of the modified meltwater runoff forcing the model at Neumayer Glacier in WB (red) and Nordenskjöld Glacier in EB (blue); (a) the volume of modified meltwater inserted (Q_p m^{3}s^{-1}) and (b) the conservative temperature (°C) (solid lines) and absolute salinity (dashed lines). Periods of the particle tracking experiments are highlighted in yellow.

Mortensen et al., 2011; Sciascia et al., 2013). The limitations of this approach are considered in Section 4.3.2.

The fully validated model configuration has been run for the 10-year period 2001 – 2010, following a 2 year spin up.

2.1. Process testing

A series of 1-year model experiments in addition to the 10-year run have been performed (Table 1). The tests are separated into those investigating a specific process, and those investigating physical scenarios linked to climate change, the flow fields of which are later used to drive the individual based model (P and CC in Table 1, respectively). Each process simulation (P) initiated on 1st January 2005 with initial conditions from the 1st January 2005 from the 10-year model output and then spun-up with the specified change in forcing for eight months to allow the model time to adjust to the perturbed forcings. The spring to winter period of September 2005 to August 2006 is examined for each process test described below. For each climate change scenario (CC), the model is spun up with the specified change for 19 months (initiated 1st January 2004), ensuring sufficient spin-up by August 2005.

Table 1
Descriptions of the process tests performed.

Name	Brief description	Process test (P) or Climate Change scenario (CC) used for particle tracking
BASE	Full validated model	P & CC
NOATM	No atmospheric forcing	P
NORNF	No meltwater forcing	P
ONLYBDY	Only open boundary forcing	P
NOWIND	No wind forcing	P
FÖHN	Föhn wind forcing	P & CC
DRNF	Double meltwater runoff	CC
HRNF	Half meltwater runoff	CC

2.1.1. Baseline experiment

The process test BASE is based on the full validated model configuration, as described in Section 2. This is the only configuration run for the full 10 years 2001–2010.

2.1.2. Removing atmospheric forcing

To test the influence of the atmospheric forcing, the process test NOATM has the bulk formulation for atmospheric forcing turned off such that all surface fluxes are set to a constant of zero.

2.1.3. Removing meltwater forcing

The test the influence of the meltwater forcing, the process test NORNF has no terrestrial meltwater forcing, such that meltwater runoff contributing to both surface runoff and the buoyancy-driven outflow is set to zero.

2.1.4. Removing atmospheric and meltwater forcing

To isolate the influence of the boundary forcing, the process test ONLYBDY combines NOATM and NORNF such that only the open boundary forcing is active. Note, it is not possible to turn boundary forcing off and maintain model stability.

2.1.5. Removing winds

To test the influence of winds alone, the process test NOWIND has the bulk formulation for all the atmospheric forcing variables turned on except for winds, which are set to constant zero.

2.1.6. Increasing the meltwater runoff

To test a scenario in which the meltwater inputs are increased due to an increase in surface melting, the volume of meltwater runoff in the theoretical climatological cycle is doubled (DRNF) before following the

process of splitting into 10 % surface runoff and 90 % subglacial discharge via the offline plume model as described above.

2.1.7. Reducing the meltwater runoff

To test a scenario in which the meltwater inputs are reduced following glaciers receding, the volume of meltwater runoff in the theoretical climatological cycle is halved (HRNF) before following the process of splitting into 10 % surface runoff and 90 % subglacial discharge via the offline plume model as described above.

2.1.8. Simulating föhn wind events

The FÖHN process test required a more involved approach based on knowledge of föhn wind events at South Georgia. The events have been hypothesised to drive differential surface melt of the island's glaciers (Bannister and King, 2015). From an oceanographic perspective, we hypothesise that föhn wind events may alter circulation and the transport of heat differentially between the fjord arms. This may have implications for both transport of biological material and submarine glacier melt. The ERA5 dataset used to force the Cumberland Bay fjord model is too coarse in resolution (~31 km horizontally) to capture föhn wind events, so in order to investigate the latter hypothesis, the ERA5 variables have been manually edited to represent regular occurrences of föhn wind events, as follows.

The criterion for the onset of a föhn event at Cumberland Bay is defined by Bannister and King (2020) as an increase in air temperature greater than 2 °C in one hour together with a marked decrease in relative humidity and a marked increase in wind speed, with wind from the direction of the island's central mountain range. The föhn conditions cease with a sudden drop in temperature. Bannister and King (2020) identified a frequency of 7.3 föhn events per month, or one event approximately every 4 days, from weather station records at King Edward Point (KEP) (Fig. 1b). For the purposes of this study, the observed mean changes in temperature, wind speed, and relative humidity for the recorded events are imposed for 24 h, every fourth day, over the course of a year. Observations show a high degree of temporal variability in both frequency and characteristics of föhn events (Bannister and King, 2015, 2020), which we do not attempt to capture in this study. The representation of föhn wind events here does not attempt to resolve specific events but captures the key observed characteristics allowing an evaluation of the potential impact of repeat föhn events over longer (yearly) time scales. The method also allows for representing how average and regular gusts of föhn winds impact larval transport and retention in spring, described below (Section 2.2). Therefore, following Bannister and King (2020; Table 3), the process test FÖHN (Table 1) assumes for each föhn event a temperature increase of 7.3 °C, a relative humidity decrease of 41 %, a wind speed increase of 10.3 ms^{-1}, a south-westerly wind direction for the three ERA5 grid cells encompassing the mountain range south and west of Cumberland Bay, and a north-westerly wind direction for the grid cell encompassing most of Cumberland Bay. This is achieved by editing the ERA5 variables for September 2005 to August 2006; outside of the föhn events, the ERA5 variables remain unchanged (Fig. 3, white arrows). The change in wind direction results in surface wind stress directed with an eastward component out of WB and a southward component into EB. The imposed pattern of wind stress (Fig. 3) agrees well with the projected 10 m wind speed and direction from a high-resolution atmospheric model of the region that considers the island's orography (Bannister and King, 2020, Figure 4b and f). However, this method does not capture the influence of föhn winds modifying freshwater inputs, which is a limitation of the model.

2.2. Individual-based model

Hourly flows for Cumberland Bay between August 2005 and January 2010 have been generated using the baseline hydrodynamic model (BASE; Table 1). This time period includes notable interannual variability in temperature and salinity (Fig. 4); for example, 2005 had a particularly cold winter, and 2009 had a particularly warm winter. This time period also overlaps with *C. gunnari* larvae sampling periods (Belchier and Lawson, 2013). For the purposes of this study, we focus solely on the hatching and subsequent dispersal period observed to have the greatest abundance of larvae, August to October (Belchier and Lawson, 2013) highlighted with white boxes in Fig. 2. Inferences for earlier hatching periods based on the identified drivers of temporal

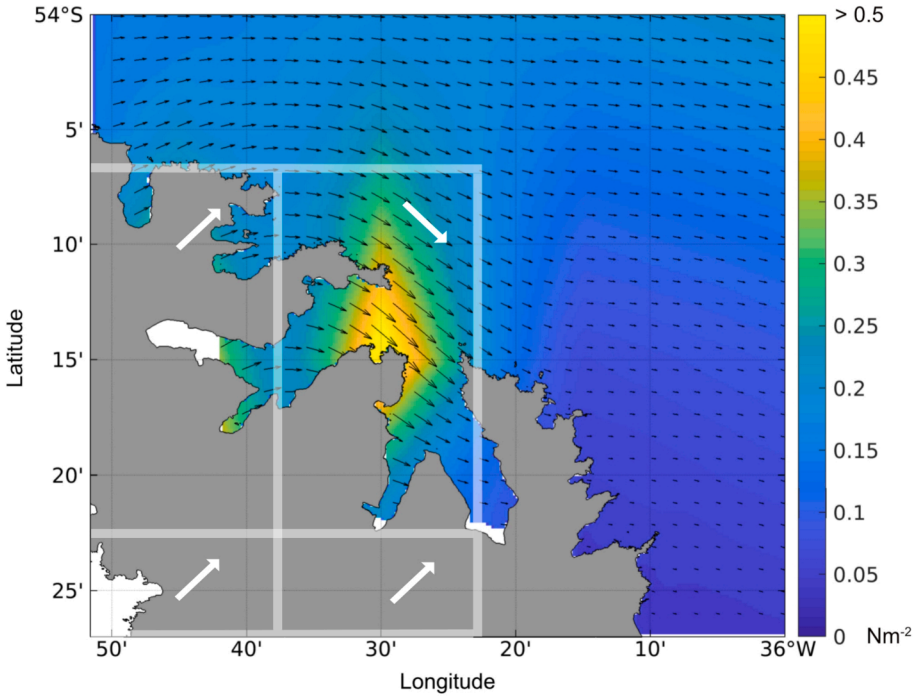

Fig. 3. An example of the 24-hour average surface downward wind stress over the model domain during a föhn wind event, demonstrating the direction of wind change. Grey boxes show the ERA5 grid cells and white arrows show the adjusted ERA5 wind directions used to represent föhn wind events.

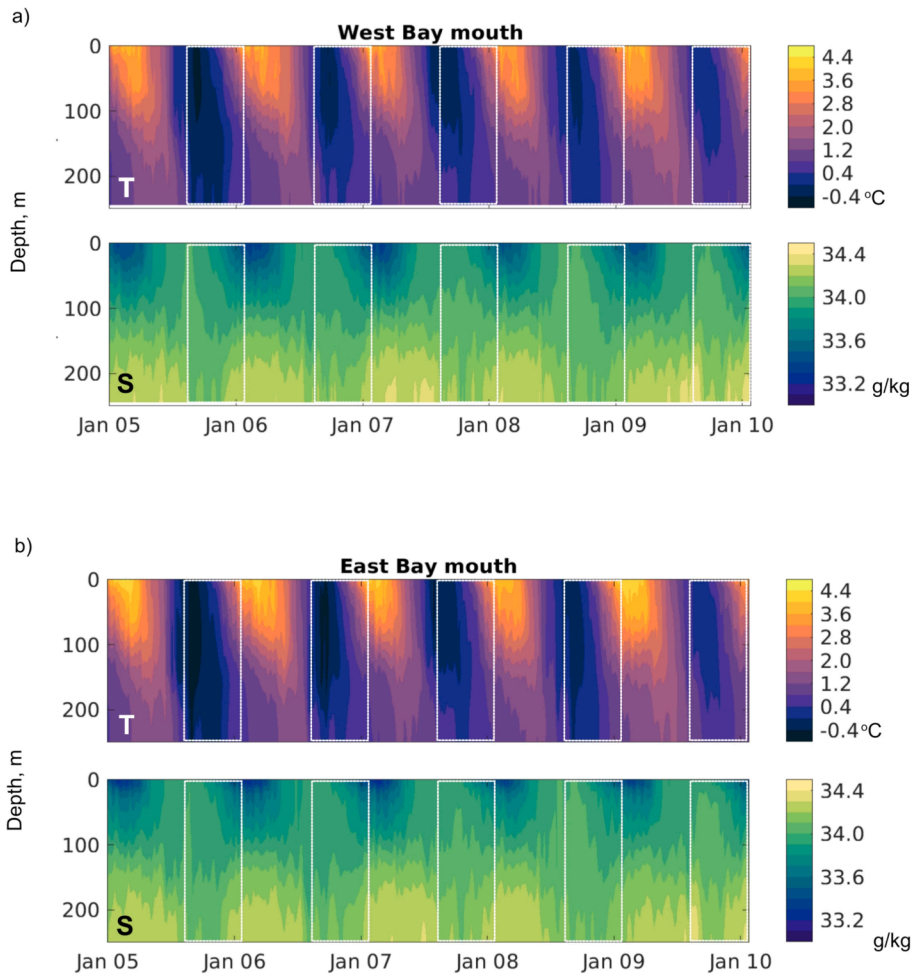

Fig. 4. Temperature and salinity at (a) West Bay fjord mouth, and (b) East Bay fjord mouth from January 2005 to January 2010. Periods with particle tracking are highlighted in white boxes.

variability in retention are elucidated in Section 4.1.

Simulated hourly flows advect Lagrangian particles representing *C. gunnari* larvae using the Hydrodynamics-based Algorithm (HAL) for Lagrangian simulations (Young, 2024) which has been used previously for modelling *C. gunnari* larvae (Young et al., 2012, 2014). The particles are parameterised to represent key aspects of *C. gunnari* larval behaviour, specifically spawning location, hatching period, observed depth range (upper 100 m) and a planktonic phase of 3 months (further details below). Particles are advected with a model time-step of 150 s, chosen based on the CFL (Courant–Friedrichs–Lewy) stability criterion (Kowalik Z. Murty, 1993), and with additional random horizontal and vertical diffusion, dh and dv, respectively (Young et al., 2012). A value of dh $= 0.1$ m^2 s^{-1} is chosen based on the criteria detailed by Okubo (1971), with a value of dv $= 1 \times 10^{-5}$ m^2 s^{-1} based on established values from observations and models (Gnanadesikan et al., 2001).

Two particles per horizontal grid cell are released at all cells within WB and EB where the bed depth is between 100 and 300 m, following literature on *C. gunnari* spawning habitats assuming benthic eggs (Kock, 1989; Parkes et al., 2000; Frolkina, 2002), totalling 4462 particles per release. As larvae have been observed to be most abundant in the upper 100 m of the water column, one particle is released at 25 m and the other at 75 m in the centre of the grid cell and restricted to the upper 100 m throughout the simulation. Particles are reflected from the upper and lower depth limits (surface and 100 m) if their predicted vertical movement would take them outside the imposed depth range. Therefore, 4462 particles, representing larvae, are released every day between 16th August – 15th October, totalling 61 releases and 272182 particles each year. These are subsequently split into 'early', 'middle' and 'late' release periods containing 21, 20 and 20 days, respectively, to assess the significance of the timing of hatching. The larval development period is assumed to be 3 months; planktonic larvae are no longer observed in the bays by mid-January (North, 2001). The particles are tracked for the duration of the assumed 3-month (90 day) larval period. A particle is considered to be retained if it remains in the vicinity of the fjord arms, or in Stromness Bay (Fig. 1b) at the end of the tracking period. The e-folding time is used as a measure of retention, calculated as the time taken (t) for the number of particles (p) in the bay to reduce to R/e, where R is the number released and e is Euler's number. The greater the e-folding time, the longer particles spend in the bay and the greater the retention rate.

Tests for the sensitivity of transport and retention of *C. gunnari* larvae to certain physical factors linked to climate change (CC, Table 1) are run for the tracking year August 2005 – January 2006 (for direct comparison to the process tests). The impact of reduced and increased glacial meltwater is tested via the HRNF and DRNF scenarios respectively, and the effect of föhn winds via the FÖHN scenario (Table 1).

3. Results

3.1. Process tests

Detailed analyses of Cumberland Bay oceanography from observations and modelling have been described previously (Zanker et al., 2024); a brief summary for context is provided here. The water column

is cold (~0 °C) and well-mixed in austral spring. Surface waters begin to warm and freshen in summer and stratification strengthens as temperatures reach a maximum near the surface (~4 °C) in autumn before cooling in late autumn, followed by weakening stratification again in winter (Fig. 2 and Zanker et al., 2024, Figure 4)). A seasonal fresh surface layer from glacial melt has been observed in late summer and autumn and high salinity identified at depth for much of the year, highest in summer. Modelled surface and 100 m flow fields have revealed a complex horizontal circulation pattern with recirculation and eddy-like features, particularly near the fjord mouth where fjord circulation interacts with the dominant northwestward shelf flows (Zanker et al., 2024, Figure 8). The width-integrated volume transport shows a dominant 4-layer structure of inflow and outflow from surface to bed for much of the year, with inflow tending toward the east of EB and south of WB, and the opposite for outflow (Zanker et al., 2024, Figure 9).

The hydrodynamic model of Cumberland Bay allows for the analysis of fjord stratification and circulation patterns, here examined as point source time-series and through the volume transported through cross sections of the fjord model (Fig. 1b, yellow dots and red dash lines respectively). We focus on the impact of the process tests on fjord temperature and volume exchange at the fjord mouth, which have direct implications for the development and transport of fish larvae.

In the ONLYBDY simulation, the water column is warmer in autumn, winter and early spring, and colder in late spring and early summer (Figs. 5b and 6b). The seasonal cycle in temperature is still apparent (not shown), albeit weaker than the BASE test. In the absence of atmospheric and meltwater forcing there is a 3-layer circulation and the surface layers (upper ~ 50 m) are dominated by inflow for much of the year except in winter (Figs. 7b and 8b). Throughout the year there is deep inflow of higher-density shelf waters that replace existing fjord waters (Figs. 7 and 8). The appearance of the deep inflow in all of the process tests suggests that near-bed flows at the mouths of the bays are driven by shelf-fjord exchange processes acting at depth at the fjord mouth and are relatively isolated from local atmospheric and meltwater influence.

The results of the NOATM and NORNF simulations suggest that in spring, atmospheric forcing is acting to cool through cold air temperatures and wind mixing, whilst meltwater forcing has little impact on the near-mouth temperature (Figs. 5c,d and 6c,d). As air temperatures and solar irradiance increase in summer, surface waters warm and the volume of meltwater forcing increases, peaking in February (Fig. 2b). The upper 200 m water column is cooled by the meltwater forcing, with the strongest impact in late summer and extending into autumn (Figs. 5d and 6d). There is a time delay between surface heating and increased meltwater inputs which gives rise to the difference in temperature pattern in ONLYBDY, illustrating the combined effect of NOATM and NORNF. The thick surface outflow is driven by meltwater forcing, via

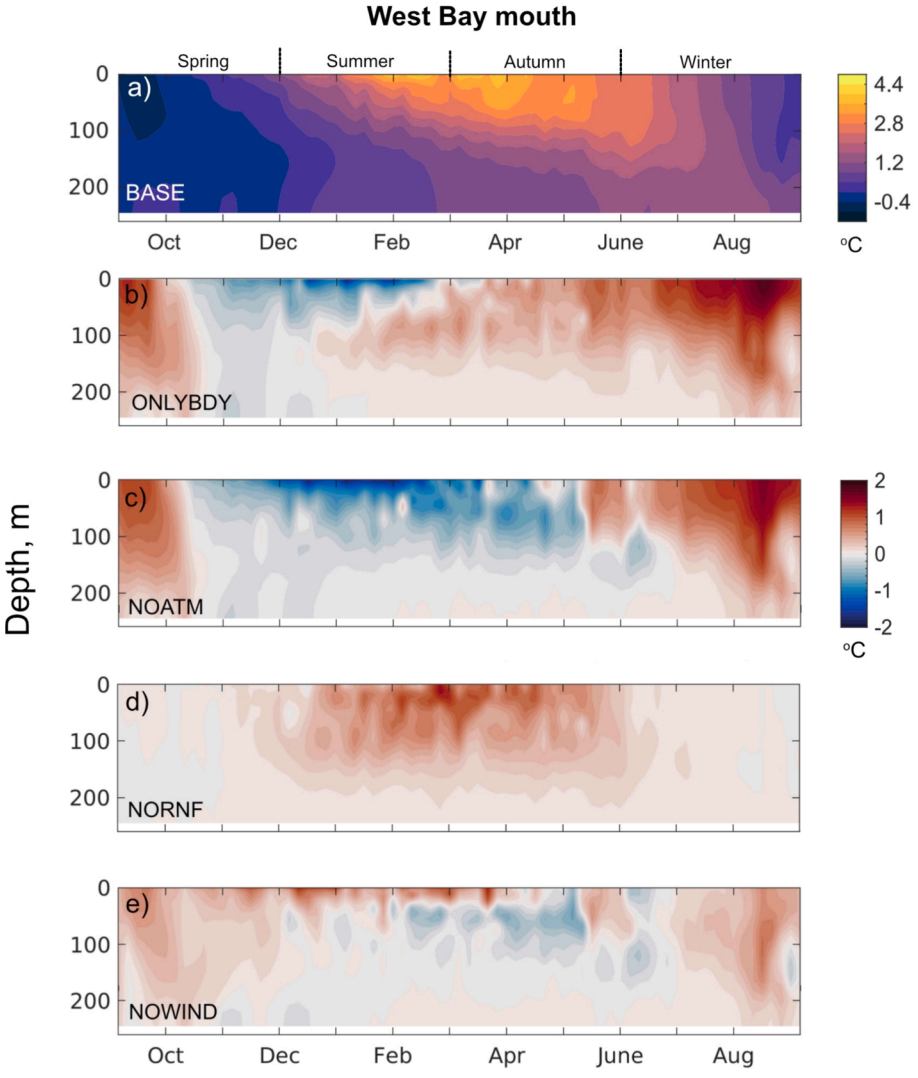

Fig. 5. (a) The BASE seasonal cycle of conservative temperature for a point in WB mouth. The difference in temperature for 4 process tests (process test minus BASE): (b) ONLYBDY, (c) NOATM, (d) NORNF and (e) NOWIND.

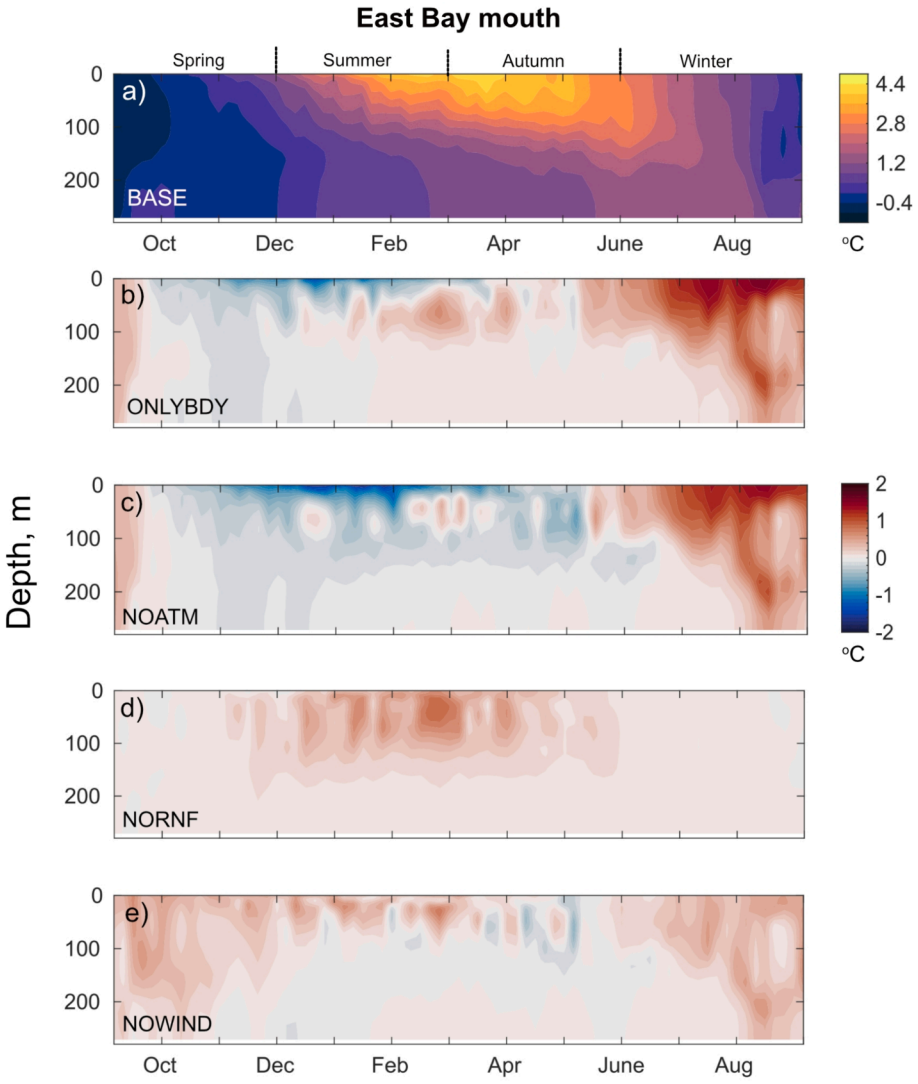

Fig. 6. The BASE seasonal cycle of conservative temperature for a point in EB mouth and the difference in temperature for 4 process tests (process test minus BASE): (b) ONLYBDY, (c) NOATM, (d) NORNF and (e) NOWIND.

buoyancy-driven outflow (Fig. 2), forming the width-integrated 4-layer structure (Figs. 7a,d and 8a,d). The atmospheric forcing warms much of the water column throughout summer and autumn through surface heating (Figs. 5c and 6c) and drives a very thin surface outflow while weakening the mid-depth intermediary exchange compared to boundary forcing alone (Figs. 7b, d and 8b,d). There is a pattern of inflow on the east, outflow on the west coast of EB, and inflow on the south and outflow on the north coast of WB, which process tests show to be driven predominantly by the atmospheric forcing, in particular winds (Fig. 9). In addition, without local forcing (ONLYBDY), predominantly north-westward shelf flows during spring to autumn drive similar patterns of outflow. With no atmospheric forcing (NOATM), or indeed just no wind forcing (NOWIND) the meltwater forcing directs outflow along the opposite coast for much of the year in WB (Figs. 9c,e).

The atmosphere is the dominant driver of warming in the upper water column in late spring and summer (by comparing NOATM and NORNF to ONLYBDY). However, by late summer atmospheric forcing is only dominant in the surface as the cooling effect of increasing melt-water inputs (Fig. 2b) becomes relatively stronger, starting subsurface and extending to the surface by early autumn (Figs. 5d and 6d). Melt-water forcing no longer impacts the fjord temperature in winter and atmospheric forcing dominates the patterns in temperature and flows.

Isolating the effect of the winds (NOWIND) demonstrates that winds have a deep cooling effect in spring and late winter by mixing the surface-cooled winter waters in both bays (Figs. 5e and 6e). Throughout summer and much of autumn, winds mix the upper layer, weakening the stratification. The dominant winds on the shelf are westerly, therefore Ekman transport will push water away from the north coast of South Georgia (northward), driving upwelling and changing density gradients between the shelf and in-fjord waters, altering exchange. Westerly winds act along-axis in WB so the effect of Ekman transport is to push flows toward the north coast, and with no wind forcing, the flows tend toward the south coast (Fig. 9e). Westerly winds act across-axis in EB and, as the fjord width is too narrow for the development of Ekman transport, winds have a weaker impact on the cross-fjord pattern of flows (Fig. 9j).

These results demonstrate how variations of flows with depth are driven predominantly by meltwater and atmospheric forcing in the upper water column, while shelf-fjord interactions are important in generating deep inflow. At mid-depth, shelf-fjord interactions are key, though modified by atmospheric and meltwater forcing. Cross-fjord variations in flow are dominated by the atmosphere, specifically winds, and by the direction and strength of the adjacent shelf flows.

3.1.1. Impact of Föhn winds on oceanographic variability

The FÖHN process test shows that with events happening every 4 days, the fjord temperatures are altered both seasonally and spatially

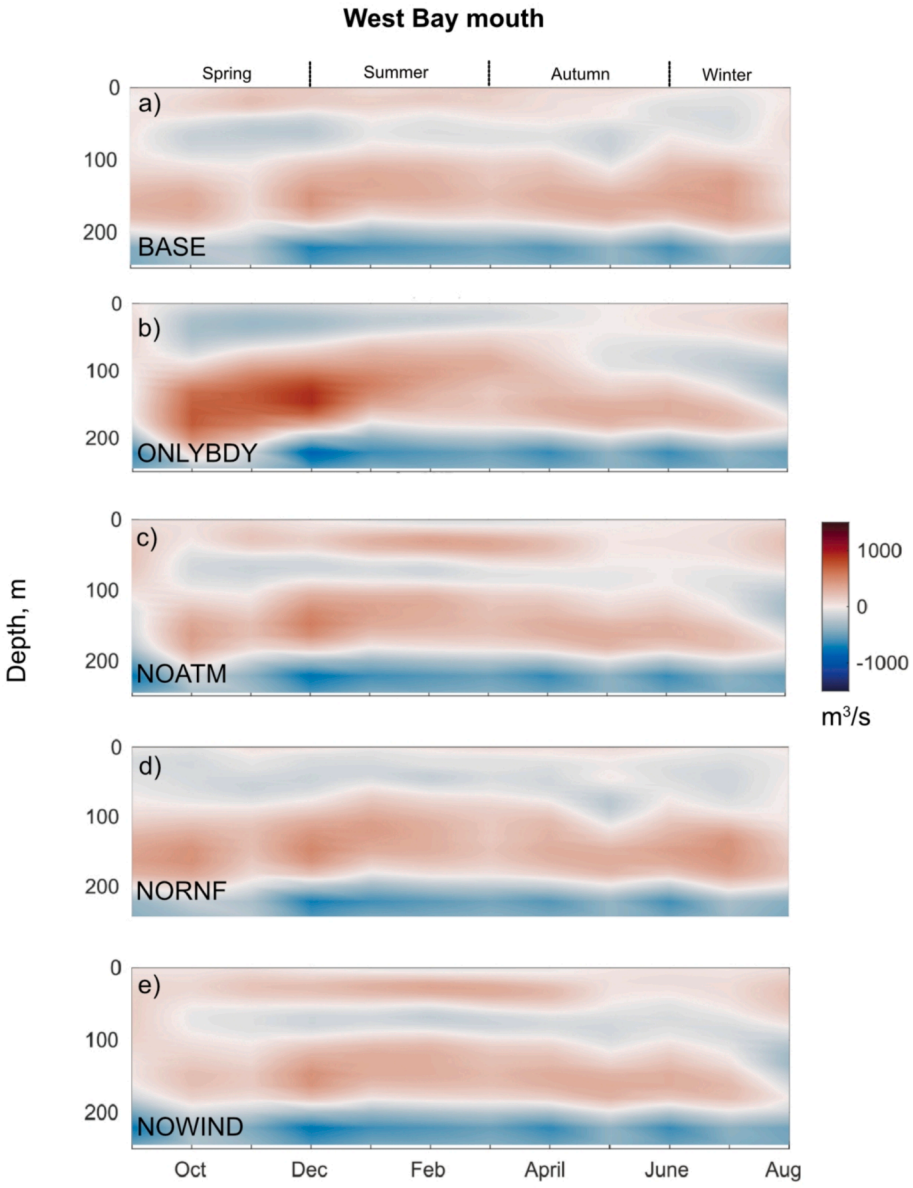

Fig. 7. (a) The BASE seasonal width-integrated volume transport (m^3s^{-1}) through a cross-section in the mouth of WB where red indicates transport out of the fjord mouth and blue indicates transport into the fjord. The seasonal transport for the process tests (b) ONLYBDY, (c) NOATM, (d) NORNF, and (e) NOWIND.

(Fig. 10). The greatest change is seen near-glacier in WB, where the mid-depth waters are warmer for most of the year, particularly in summer and autumn, though the near-surface waters are cooled during the latter period (Fig. 10c). In EB, however, the near-glacier mid-depth waters are colder in summer, autumn, and winter, with patches of warming in spring (Fig. 10d). The flow fields show that throughout the year, the föhn events increase the speed of the surface outflow along the north coast of WB (Fig. 11e-h). In summer there is a broad cooling of the sea surface temperature (SST). As the FÖHN process test increases air temperature, the cooling can be attributed to increased wind-driven mixing in the upper water column. The SST in WB is greatest in autumn, due to the higher seasonal air temperatures, further increased by föhn events. Conversely, föhn wind events result in a reduction in flows out of EB in spring and summer with an associated slight increase in SST, particularly towards the glacier terminus. In autumn and winter flows are directed cross-fjord and SSTs are broadly reduced in EB, potentially due to föhn wind-induced up- and downwelling (Fig. 11i-l).

3.1.2. *Spatial variability*

Comparing WB and EB, the effect of atmospheric and meltwater forcing shows largely the same seasonal impact near the mouths of the bays, although previous work has shown that near-glacier, there are clearer differences in the impact of drivers on seasonal temperature variability (Zanker et al., 2024). The meltwater forcing has a stronger cooling effect lasting further into the year in WB compared to EB where atmospheric warming is dominant year-round. These differences can be largely attributed to the difference in plume dynamics due to the different depths of the theoretical glacier grounding line (Zanker et al., 2024). The buoyancy-driven outflow is stronger in WB, having upwelled deeper colder waters adjacent to Neumayer Glacier, and drives subsurface outflow near-glacier on the north coast in autumn, whilst EB shows a more estuarine-like circulation due to the shallower grounding line and weaker buoyancy driven outflow (Figs. 2, 7 and 8). Winds have a strong impact on the cross-fjord structure of flows in WB and a weaker impact on the cross-fjord structure in EB, attributed to the different orientation of the fjord arms with respect to the winds (Fig. 9). When strong northwesterly winds are periodically forced over the bay and

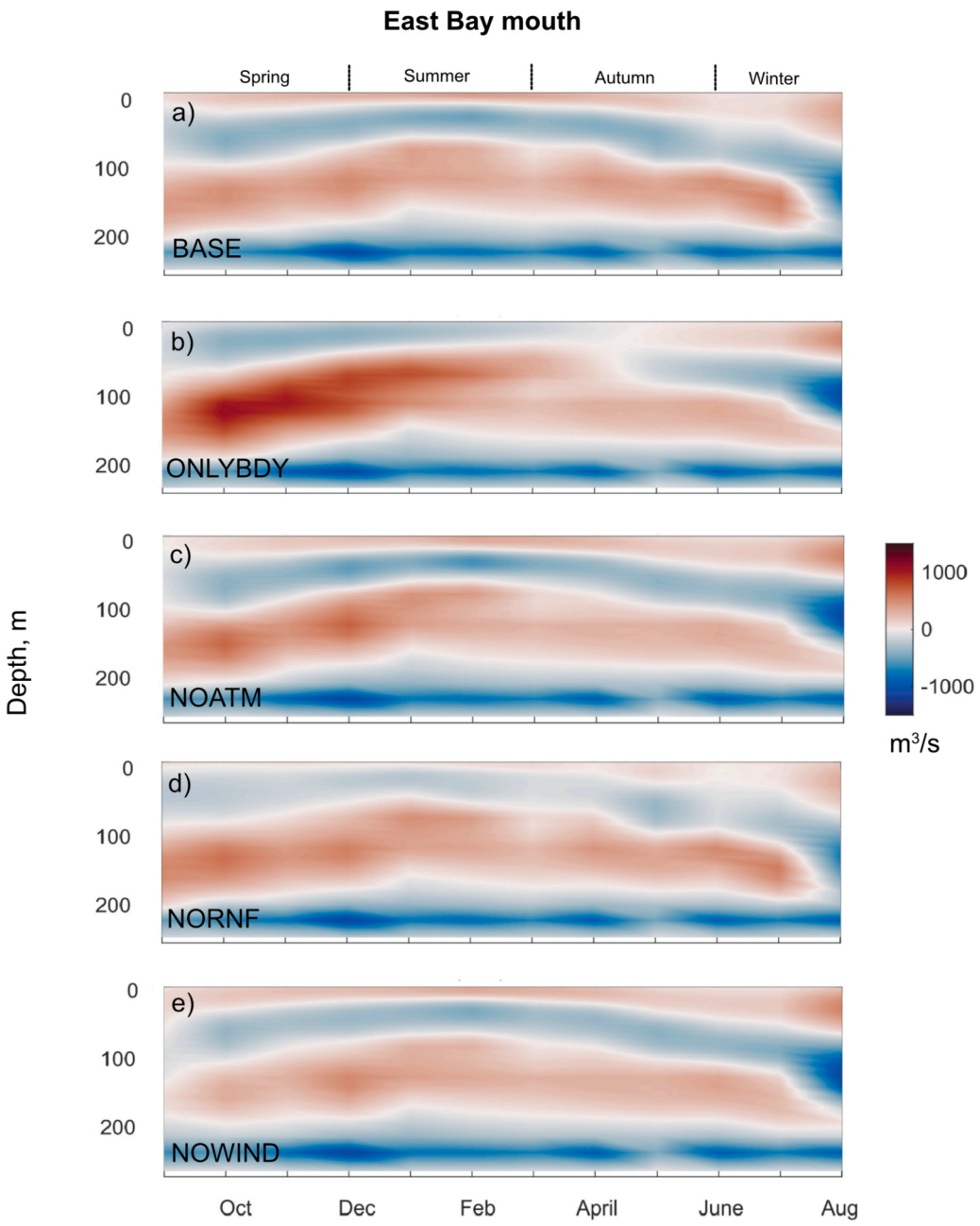

Fig. 8. (a) The BASE seasonal width-integrated volume transport (m^3s^{-1}) through a cross-section in the mouth of EB where red indicates transport out of the fjord mouth and blue indicates transport into the fjord. The seasonal transport for the process tests (b) ONLYBDY, (c) NOATM, (d) NORNF, and (e) NOWIND.

southwesterly winds are forced over the mountains to the south of the bay (FÖHN), WB experiences an increase in surface outflow while EB experiences an increase in cross-fjord flows (Fig. 11a-h).

3.1.3. Interannual variability

The interannual variability in temperature and salinity can be examined for the 5 years 2005 – 2009 of the BASE experiment (Fig. 4). The winter and spring of 2005 are notably colder deeper in the water column than the later years, whilst 2009 is the only year where winter and spring temperatures do not reach below zero. There is higher salinity near surface for the winter and spring of 2009 compared to the previous 3 years, and 2007 and 2009 see higher salinity at depth (Fig. 4).

The drivers of the interannual variability can be inferred from the process test results described previously. As the hydrodynamic model uses a climatological freshwater cycle, there is no interannual variability in the volume of freshwater inserted as either surface runoff or subglacial discharge, leading to only small interannual variability in the meltwater forcing via the plume parameterisation (due to variability in the ambient ocean properties) (Fig. 2). This is reflected in the modelled 5-year temperature and salinity profiles for summer and autumn (Fig. 4). The greatest variability between years is seen in winter and spring (June to November), which is shown above to be dominated by atmospheric forcing, in particular winds, of the upper water column. Monthly averaged 2 m air temperature from the ERA5 dataset covering Cumberland Bay (Fig. 3, top right white box) shows some interannual variability in the local atmospheric forcing (Fig. 12). The higher air temperatures in spring and winter of 2008 and 2009 are reflected in the ocean model. The variability in precipitation, such as the high precipitation in autumn of 2005, is not clearly reflected in the ocean model suggesting its impact is small compared to other processes affecting

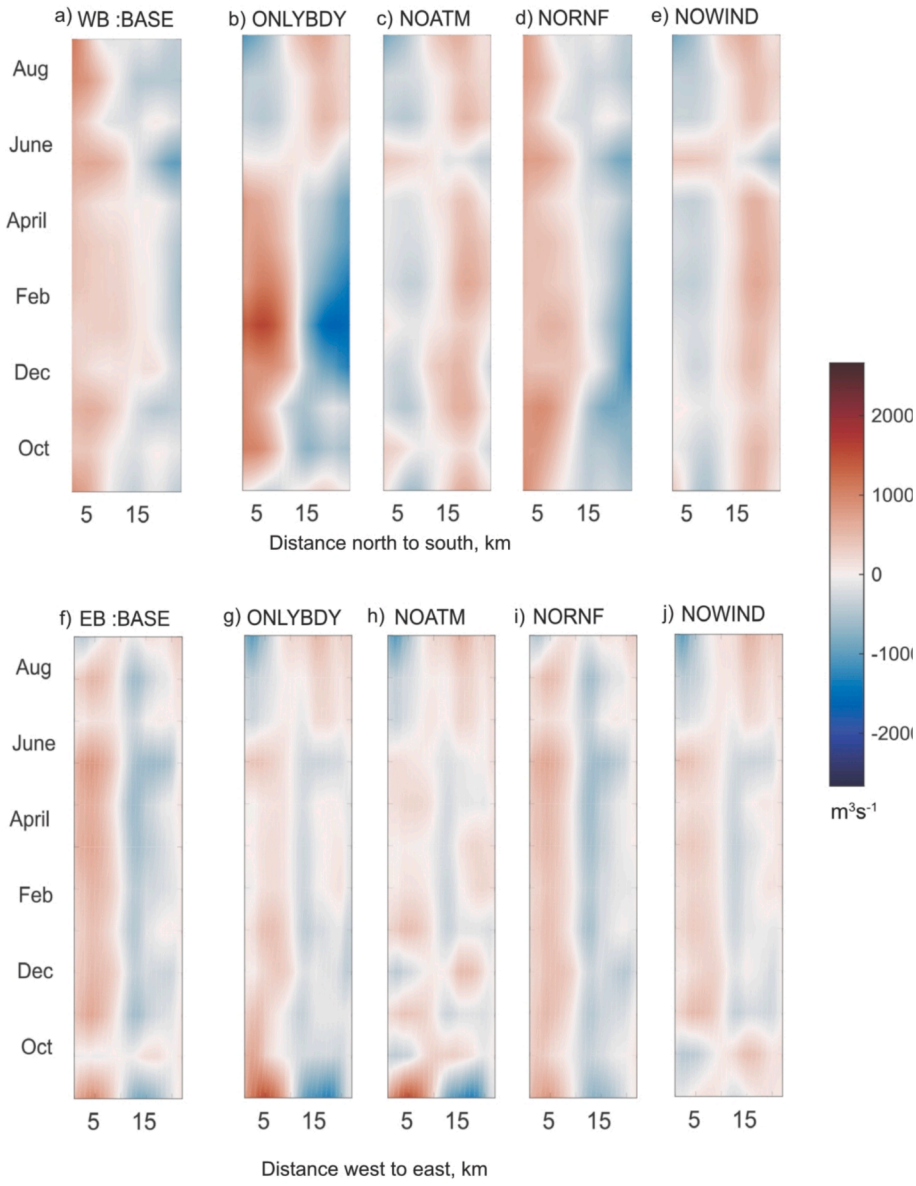

Fig. 9. The seasonal depth-integrated volume transport (m^3s^{-1}) through a cross-section in the mouth of WB (a – e) and EB (f – j) for BASE, ONLYBDY, NOATM, NORNF and NOWIND process tests, where red indicates transport out of the fjord mouth and blue indicates transport into the fjord.

salinity (Fig. 12a). The variability in salinity in the deeper water column is influenced by shelf exchange and variability in the wider ocean circulation. The high wind speeds in summer and autumn of 2005 may have had a delayed effect on cooling the water column in the following spring due to increased surface cooling through evaporation and stronger vertical mixing (Fig. 12b). However, the lack of clear correlation between variability in the ERA5 data and the ocean model variability suggests that interannual variability is driven by more remote oceanographic and atmospheric conditions that are captured in the regional model used to derive the ocean boundary forcing.

3.2. *Individual-based modelling*

Over the 5 tracking years, 4462 particles are released (2056 in EB and 2406 in WB) each day, and the total retained for each daily release over the 5 years varies from 3 to 87, or 0.1 to 2 % (Fig. 13a), as most particles are flushed out of Cumberland Bay onto the shelf. The potential fecundity of *C. gunnari* is ~1500 to 31,000 eggs per fish each season, so each model particle represents potentially thousands of individual larvae; therefore, the percentage retained still represents a considerable number of larvae, based on the limited knowledge we have of the abundance of *C. gunnari* in the bay. There is relatively strong interannual variability in the number retained, particularly in WB (Fig. 13a). The years 2005 and 2006 have the greatest number of successfully retained particles overall, with 2007 and 2009 having notably fewer. A few particles are transported to Stromness Bay (location labelled in Fig. 1b), considered here to examine the potential for downstream recruitment, where they remain for the remainder of the tracking period. There is no consistent pattern across the years for the impact of the timing of release on the number retained, for example, 2006 and 2008 see an increase in the number retained for later releases, but 2007 and 2009 do not follow this trend (Fig. 13a).

The e-folding time also shows some interannual variability but no consistent relationship between e-folding time and release period (Fig. 13b). Excluding the transport of particles between bays, WB and EB generally show the same e-folding time pattern throughout the time series, and WB tends to have slightly longer e-folding times (Fig. 13b). When transport between bays is included, WB has a consistently greater

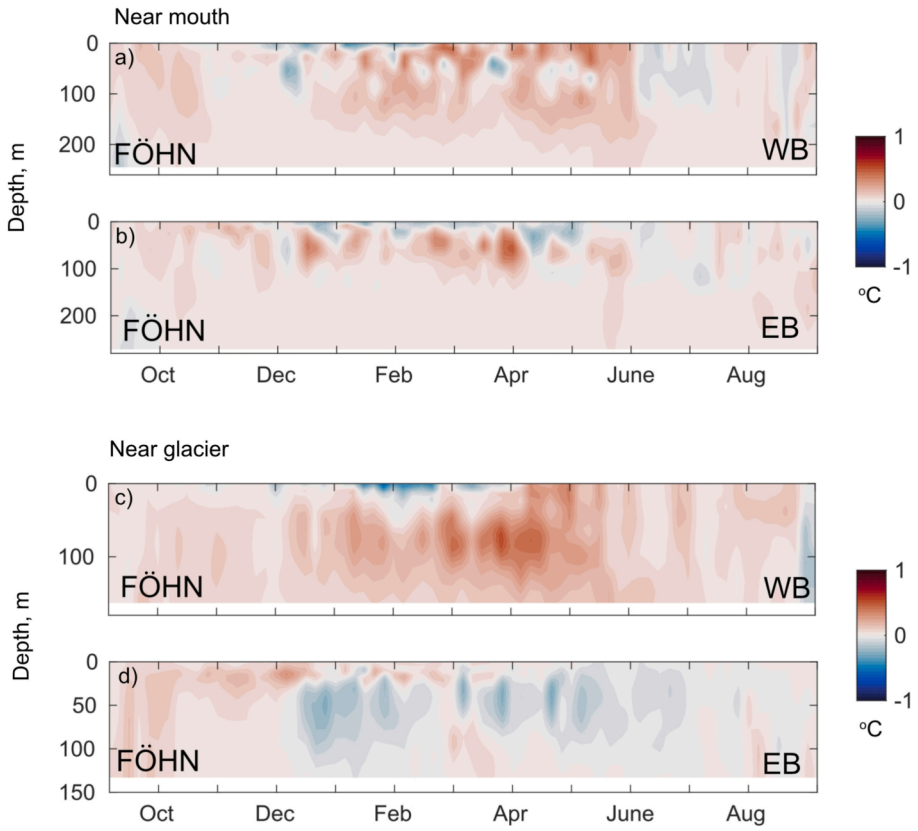

Fig. 10. The difference in conservative temperature between the BASE run and the process test FÖHN (test minus BASE) at a point in (a) WB and (b) EB mouth, and (c) WB and d) EB near-glacier (yellow dots Fig. 1b).

e-folding time (due to replenishment from EB), while EB is unchanged, demonstrating that a considerable number of particles that are flushed out of EB enter WB, but not vice versa (Fig. 13b). The cumulative particle densities show that a higher number of particles are retained from the mid (5th September to 24th September) and late (25th September to 15th October) release periods, with a greater number of those retained having started in WB (Fig. 14b, c). Overall, WB appears to be the more significant spawning and retention zone, though particles that start in EB may be retained in WB. This highlights the importance of geographical location for retention, as found in a previous study of larval transport in the wider South Georgia region (Young et al., 2012). The timing of hatching appears to be important for magnitude of retention but not for the distribution (Fig. 14).

Frequency of wind direction during the particle tracking period does not appear to correlate with the number of particles retained. For example, the 2006 and 2007 had a very similar frequency of wind from the northwest (Fig. 12c), but show the greatest difference in the numbers retained, and different e-folding time patterns (Fig. 13). Neither is there a consistent relationship between e-folding time and the wind speed over various time scales (statistical tests not shown).

The depth at which the particle is released does has a significant effect on retention with the majority of retained particles released at 75 m, rather than 25 m (not shown). This is due to the increased likelihood of shallower particles being flushed out by the surface outflow, which dominates the upper ~ 50 m (Figs. 7a and 8a). As the strength and depth of this surface outflow varies in time and between fjord arms, this suggests that larval retention is sensitive to the timing of hatching and the larval depth, with implications for larvae undergoing diel vertical migration discussed further in Section 4.3.1.

3.2.1. *Impact of physical variability linked to climate change*

The results of the particle tracking simulations demonstrate how variability in the oceanography of Cumberland Bay can drive interannual variability in larval retention, with freshwater and atmospheric forcing identified as key drivers of variability, further impacted by variability in the wider shelf oceanography. To understand how larval retention may be impacted by a changing climate, the particle tracking for releases in 2005 is repeated with hourly flow fields from three of the climate change scenario tests (Table 1): a representation of föhn winds (FÖHN), and halving (HRNF) and doubling (DRNF) the volume of meltwater input.

With DRNF flow fields, the e-folding time in WB increases for the mid to late release period but decreases for the latter half of the late release period when the stronger surface outflow (Fig. 2) increases particle export compared to the baseline volume of meltwater (Fig. 15a). The associated retention for DRNF is higher for early releases and drops steadily towards lower levels of retention than the BASE simulation for late releases (Fig. 15a). The increase in e-folding time for the mid release period (compared to BASE) is not coincident with an increase in retention suggesting that the increase in meltwater forcing is increasing recirculation in the bay, but ultimately flushing more particles out before the end of the 90-day tracking period. The higher numbers of particles retained in WB for the early release period is due to an increase in the number of particles released in EB entering WB, particularly in the upper 25 m (Fig. 16c). The HRNF test shows the opposite pattern to DRNF for retention in WB, although the e-folding time is very similar to the BASE simulation (Fig. 15a), as the meltwater forcing is relatively low for BASE in the first 30 days (Fig. 2). The numbers retained in WB increase for later release days, as more particles from EB enter WB and fewer particles are exported by the weaker buoyancy-driven outflow (Fig. 15a). EB is less impacted by the change in the volume of meltwater as the buoyancy-driven outflow is weaker and has a more limited depth range than in WB (Fig. 2). For particles released at 25 m in EB, more circulate around EB with reduced meltwater leading to longer e-folding

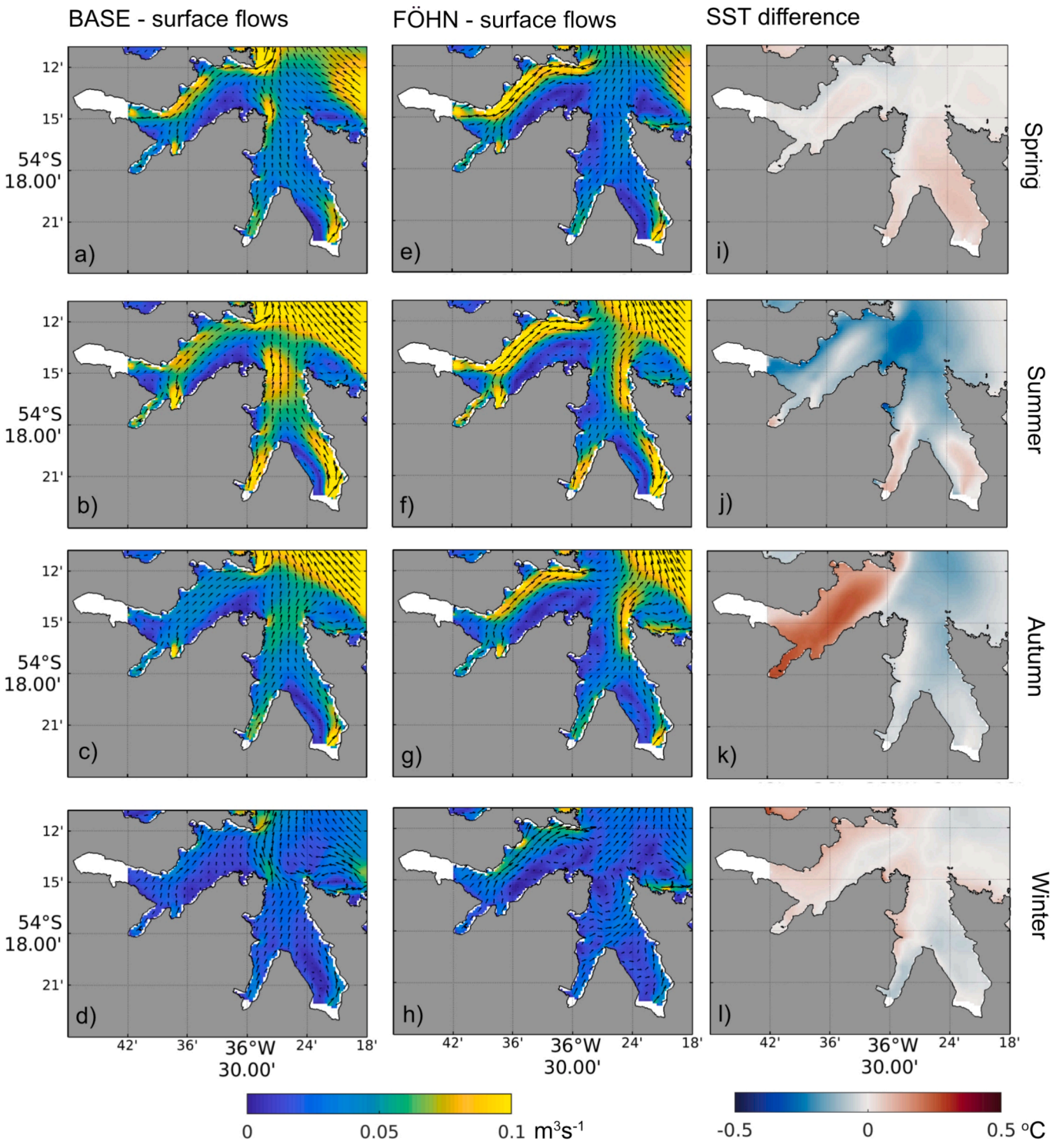

Fig. 11. Seasonal (as labelled) 3-month averaged (a-d) BASE surface flow, (e-h) FÖHN surface flows, and i-l) the difference in SST (FÖHN minus BASE).

times for late releases, and fewer circulate around EB when meltwater is increased due to the enhanced surface outflow (Fig. 16 c, d, g, h). The results here highlight the importance of timing of hatching in relation to the meltwater forcing cycles. In all cases, the plume does not reach neutral buoyancy sub-surface during the tracking period, so the effect of a sub-surface buoyancy-driven outflow on particle transport is not demonstrated here.

The results presented in Section 3.1.1 demonstrated how föhn wind events drive spatially different oceanographic conditions between the fjord arms. Repeating particle tracking with flow fields from the FÖHN process test similarly shows spatially different responses. A strong northwesterly wind drives recirculation in WB and a cross-fjord flow in EB induces upwelling on the west coast, due to the orientation of the arms with respect to the wind. For WB, the e-folding time and number retained are similar to the BASE run (Fig. 15a, b), however, there are notable differences in the underlying patterns of particle transport. Far more particles circulate near the mouth of WB, but fewer towards the head, and fewer particles enter from EB into WB for the FÖHN test due to

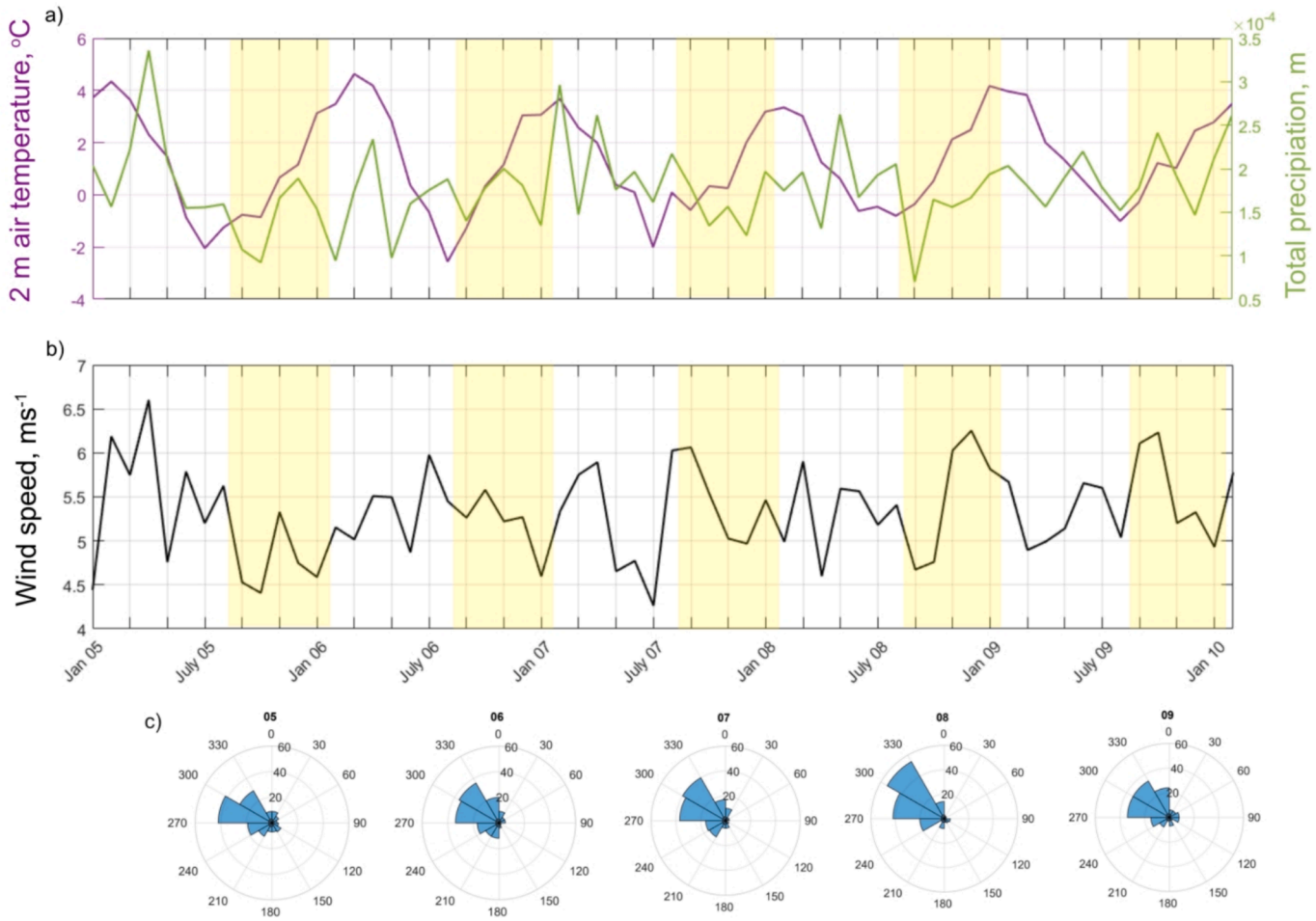

Fig. 12. ERA5 (a) 2 m air temperature and total precipitation and (b) wind speed for the grid cell best representing Cumberland Bay between January 2005 to January 2010. The periods overlapping with particle tracking experiments are highlighted in yellow. (c) the frequency of ERA5 wind direction for the same grid cell during the particle tracking experiments; 30° bins show the direction from which the wind is coming.

the change in near-surface flows (Fig. 17). So, while more particles released in WB may remain in WB, fewer are being transported from EB, resulting in similar numbers retained after 90 days compared to the BASE run. In EB, however, the number retained doubled for most release days (Fig. 15b). This is due to more of the particles released in EB circulating around EB, particularly those released at 25 m, due to the impact of winds acting across the fjord (Fig. 17).

The results of the DNRF, HRNF and FÖHN simulations show that both the volume of meltwater runoff and the frequency/intensity of föhn wind events have the potential to impact the number of larvae retained in Cumberland Bay. In general, retention after 90 days reduces with increased volumes of meltwater runoff. However, this pattern is less clear for early releases at the end of winter when meltwater volumes are low and weak buoyancy driven circulation interacts with strong winter wind-driven circulation. Föhn winds have a spatially varying impact between the fjord arms, generally increasing retention after 90 days in EB, and reducing retention after 90 days in WB due to the orientation of the arms with respect to the wind direction. The impact of these factors is sensitive to the timing of hatching, particularly in the case of the volume of meltwater runoff. The implications for different biological characteristics, including spawning times, alongside physical oceanography are discussed further in Section 4.

4. Discussion

4.1. Temporal and spatial variability in circulation and larval retention

The results of the process tests suggest that the key drivers of temporal and spatial variability depend on the season, which has direct implications for the timing of release (hatching) of icefish larvae in Cumberland Bay. The August larval pulse considered in this modelling study is assumed to be the largest based on limited studies (Belchier and Lawson, 2013). The subsequent 90-day dispersal period encompasses late winter and spring when meltwater forcing is less dominant, and the interplay is between the atmospheric and boundary forcing (Section 3.1). At depth, the boundary forcing drives dense coastal inflow throughout the year and complex intermediary mid-depth exchange, which is modified by the winds. This is illustrated by the relatively strong interannual variability in retention but lack of consistent pattern between the years for the timing of release versus the number retained. Winds can vary on short timescales and interact with the upper water column impacting ecological processes in the fjord, as seen in the Antarctic Peninsula (Lundesgaard et al., 2019). Wind conditions could strongly influence variability in retention if they drive recirculation features. The results described in this study agree with previous studies on the complex impact of winds and meltwater on zooplankton dispersal, illustrating how changes in wind conditions and meltwater runoff timing and volume could alter coastal ecosystems in the future (Arimitsu et al., 2016; Ziegler et al., 2020).

There is clear modelled and observed seasonality in circulation in

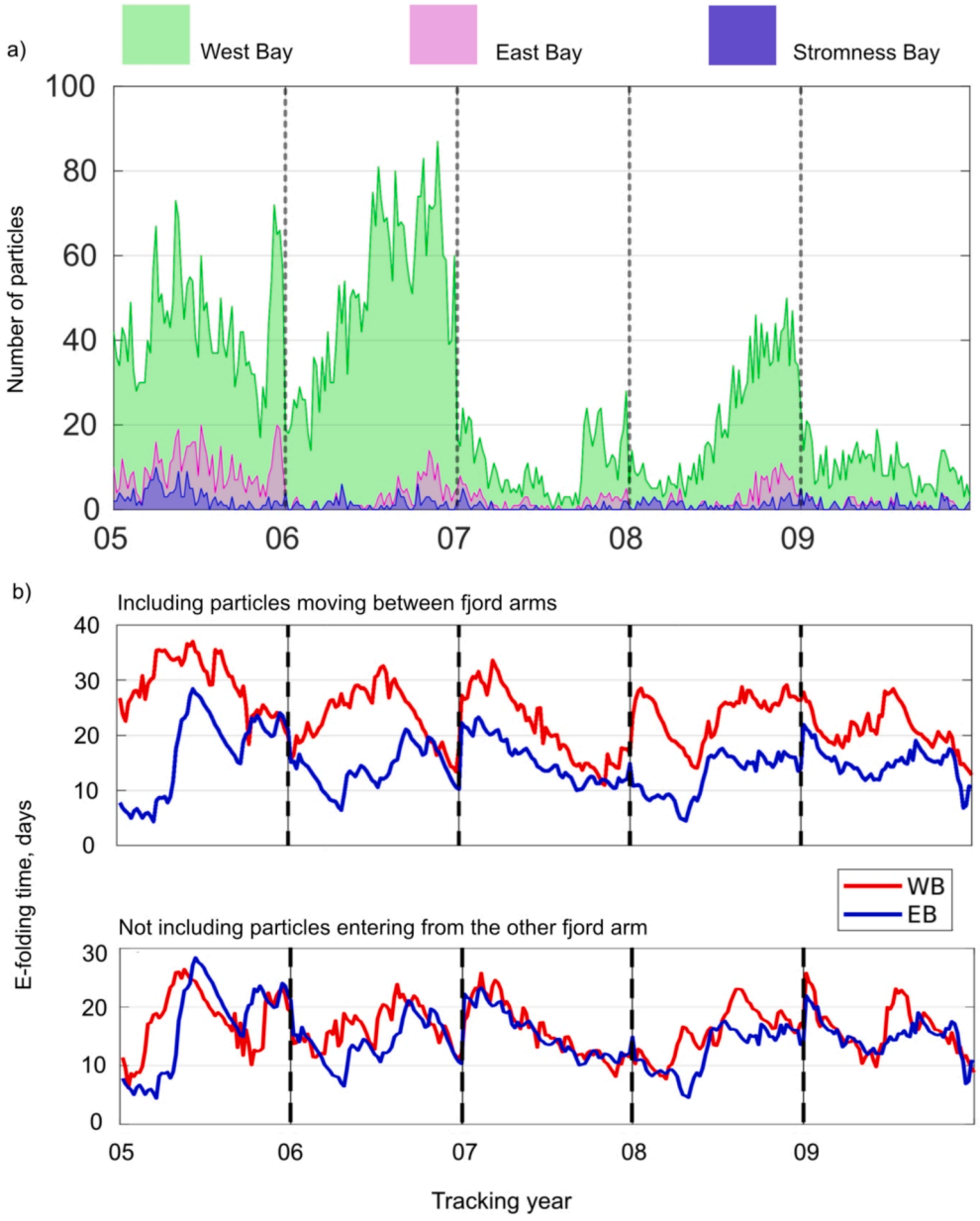

Fig. 13. (a) The total number of particles in the bays after 90 days of tracking for 61 release periods for each of the 5 years of tracking, separated by whether the particles ended in West Bay, East Bay or Stromness Bay. (b) The e-folding time for each release period for particles in WB (red) and EB (blue), separated into being calculated by including particles moving from one fjord arm into the other, and by not including particles entering from the other fjord arm, as labelled.

Cumberland Bay, so if *C. gunnari* larvae were to hatch at a different time of year, the key drivers of transport and chances of retention are likely to be different. There is evidence to suggest a high larval abundance also appears sporadically in June (Belchier and Lawson, 2013). The water column is warmer in June with residual stratification following summer surface heating and freshwater runoff (Figs. 5a and 6a). The glacial meltwater runoff is at its lowest from June to August, and the outflow plume may terminate sub-surface in WB (Zanker et al., 2024; Fig. 3e). This is likely to increase retention, especially for larvae in the upper 50 m, but may cause deeper larvae in WB to be exported by the subsurface outflow. The timing of hatching and the length of planktonic phase, particularly in relation to the volume of meltwater runoff, is therefore very important for understanding the potential retention success of a cohort of icefish larvae.

The geographical location of release (spawning/hatching) of *C. gunnari* larvae has also been found to be key to the chances of successful retention. Overall, WB appears to be the more significant spawning and retention zone, though particles that start in EB may be retained in WB. Stromness Bay does not appear to be a significant retention zone. Section 3.1.2 and previous work (Zanker et al., 2024) found there to be spatial variability in the circulation between fjord arms. Notably, buoyancy-driven outflow affects a deeper portion of the upper water column in WB compared to EB, especially near-glacier (Zanker et al. 2024, Fig. 10). In general, process tests find the circulation in WB is influenced by the combined effect of winds and buoyancy-driven outflow, whilst EB is characterised by an estuarine-like circulation with winds having a weaker influence in summer and autumn (Section 3.1.2). Therefore, the location of spawning (WB or EB), and subsequent hatching, is an important factor for chances of retention. In the 5 years of model simulations, overall the highest portion of those retained had been released in WB, though this may be impacted by the timing of spawning and potential changes in climatic conditions.

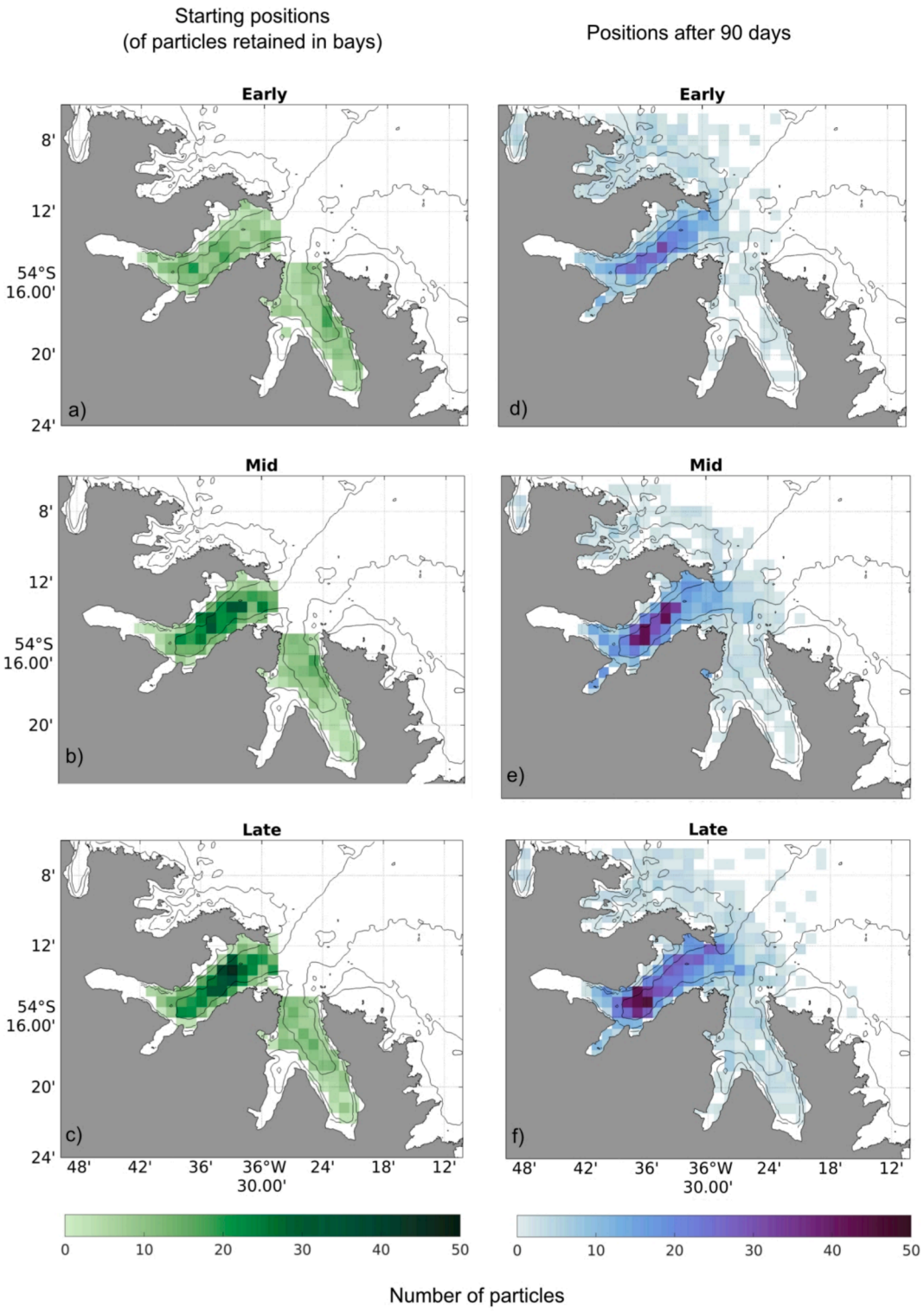

Fig. 14. 2005—2009 cumulative particle densities for early (August 16th- September 5th), mid (September 6th- September 25th) and late (September 26th- 15th October) particle releases. (a) – (c) Starting position for all particles retained in West Bay, East Bay and Stromness Bay and (d) – (f) locations of all particles after 90 days of tracking.

Interannually, the retention of ice-fish larvae could vary significantly. Results presented in Section 3.1 showed that atmospheric forcing is the main driver of variability during the modelled dispersal period (winter and spring). Since the meltwater forcing has very little interannual variability in the model and is not a dominant driver during this time, this suggests the interannual variability in retention may be wind-driven. However, no consistent pattern is found between e-folding time and the frequency or wind direction for each year, neither is there a consistent relationship between e-folding time and the component of the wind or wind speed over various time scales. The results of the process tests find variability in fjord circulation is driven predominantly by meltwater and atmospheric forcing in the upper water column, and at mid-depth shelf-fjord interactions are key, though modified by atmospheric and meltwater forcing. Cross-fjord variations in flow are

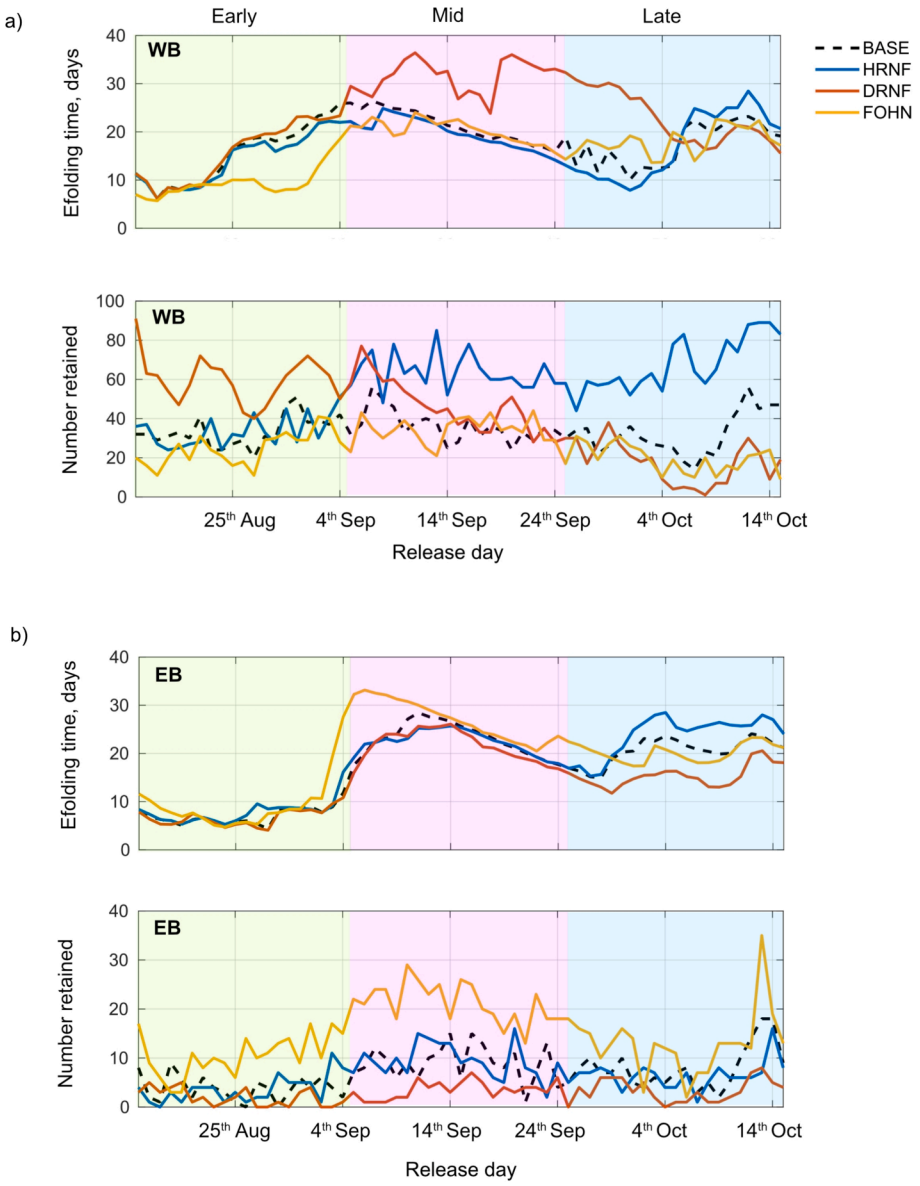

Fig. 15. The e-folding time (top panel) (excluding particles transported from one bay to the other) and the number of particles remaining in the bay after 90 days (bottom panel) for a) WB and b) EB, for the HRNF, DRNF and FOHN tests. BASE run is in black dashed lines.

dominated by the atmosphere, specifically winds, and by the direction and strength of the adjacent shelf flows. Therefore, the interannual variability in particle retention is likely due to a complex interplay between these drivers that is not trivial to separate. Along-fjord winds out of the bay may increase the export of particles near the surface, but draw in deeper particles due to the compensating sub-surface inflow. Cross-fjord winds may cause up- or downwelling near the coast, changing the depths of the particles and thus altering chances of retention. The combination of wind direction and boundary flow may also drive complex exchange and recirculation features near the fjord mouth that could act to entrap particles for longer, increasing the chances of retention. The shelf circulation has been shown to exhibit strong interannual variability driven by regional wind stress and the more remote influence of the SACCF (Combes et al., 2023). As salinity is notably higher at depth in 2007 and 2009 (Fig. 4), this suggests that variations in shelf flows and water mass characteristics contributed to a change in circulation leading to reduced retention. Higher salinity waters at depth could be expected to enhance estuarine circulation with the increased outflow in the upper water column leading to lower retention.

The first 4 years (2005 to 2008) of the simulation period in this study overlap with larval abundance surveys in Cumberland Bay (Belchier and Lawson, 2013). Belchier and Lawson (2013) analysed ichthyoplankton data collected year-round and long-term to assess variations in larval fish diversity and abundance. The study found significant interannual variability in the larval fish assemblage. In particular, they found higher larval abundances in 2005 and 2006 compared to 2007 and 2008, which broadly agrees with our model results of larval retention (Fig. 15a), suggesting that the underlying oceanography may be a key driver of variability in larval abundance. However, there are many other factors that impact larval abundance discussed in Section 4.3.1, which challenge the reliability of this comparison.

4.2. *Influence of physical processes linked to climate change*

The results from Section 3.1.1 showed that the circulation in WB responds differently to the regular occurrence of föhn wind events than the circulation in EB. Much of the water column is warmed in WB for the majority of the year, most notably in autumn, whereas there is a

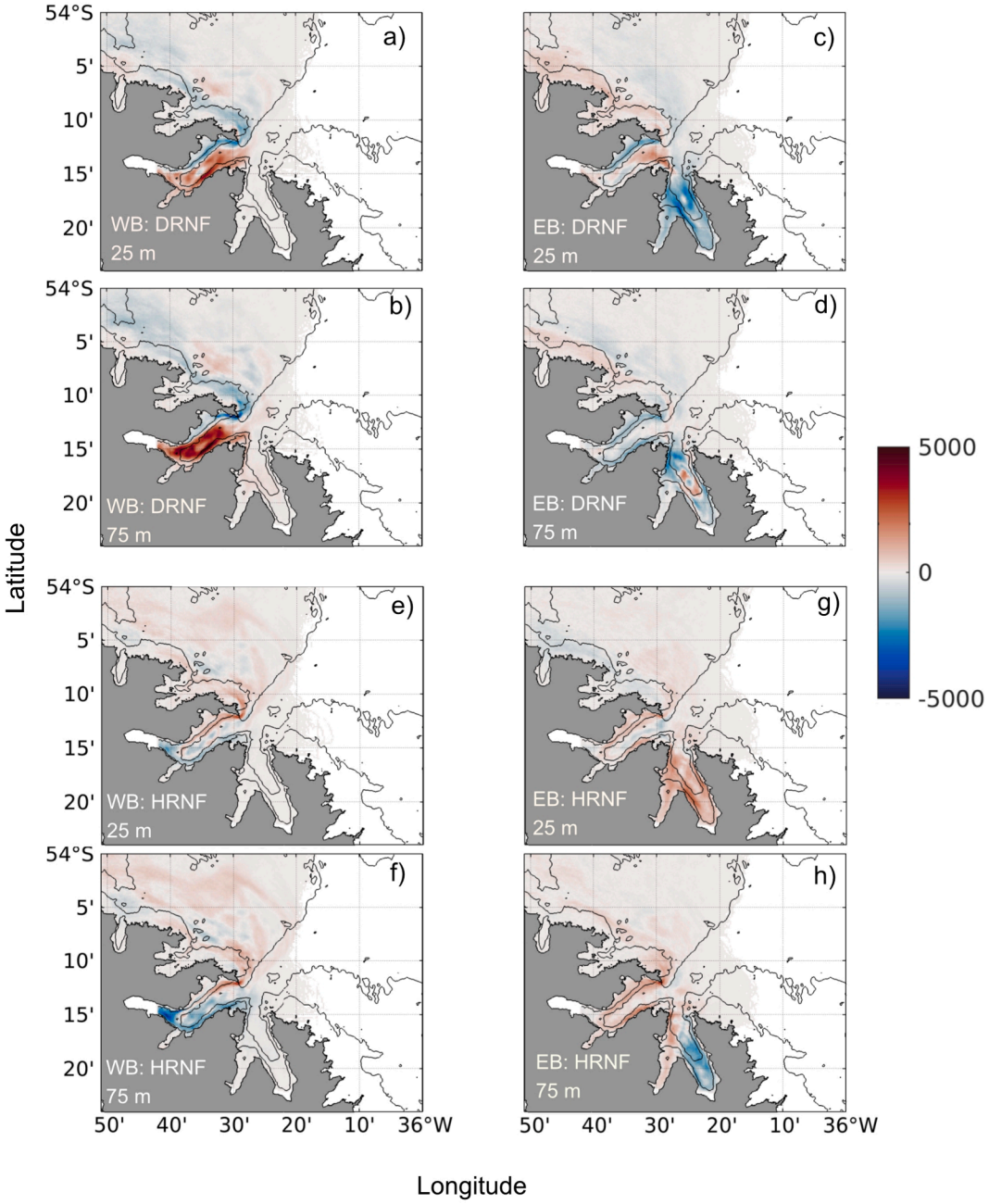

Fig. 16. The difference (test minus BASE) in the number of particles passing through each model grid cell between the BASE run and (a) – (d) DRNF, and (e) – (h) HRNF, separated into WB (left), EB (right), 25 m releases (above) and 75 m releases (below), as labelled.

shallower response in EB (Fig. 10). Similarly, in autumn, sea surface temperatures are increased in WB, but reduced in EB (Fig. 11i–l). Additionally, the periodic changes in wind direction over the fjord generate complex circulation patterns including eddies and cross-fjord flows, resulting in stronger fjord-wide horizontal circulation (Fig. 11e–h). The increase both in temperatures and horizontal circulation can be inferred to provide more energy for submarine glacial melt. Föhn winds are also likely to increase the surface melt of Neumayer Glacier through the increase in air temperature, but to a lesser extent for Nordenskjöld Glacier due to the orientation of the glaciers with respect to the wind direction (Bannister and King, 2015). The increase in surface melting may decrease the mass balance of Neumayer Glacier as well as increase the volume of meltwater runoff, with implications for larval transport.

In the short term, as glaciers retreat rapidly, there will be an increase in glacial meltwater runoff. As this is a seasonal driver, the influence of this on larval retention strongly depends on the time of hatching. Most significantly, for larvae hatching in August the model finds increased runoff can increase retention, while fewer are retained for those hatching in October. The influence varies between fjord arms due to the differing bathymetry and buoyant plume dynamics. In the longer term, as glaciers continue to retreat and thin, the volume of meltwater runoff would decrease, which the model suggests would lead to higher retention for later releases (September and October). If the glaciers were to retreat onto land, buoyancy-driven outflow would cease, and there would only be a thin surface outflow from the surface freshwater runoff. This is likely to have a very strong impact on retention; the e-folding time would likely increase significantly due to much weaker outflow, such that there would be far more successful retention of larvae spawned in Cumberland Bay. In fact, due to the rapid retreat of Neumayer Glacier

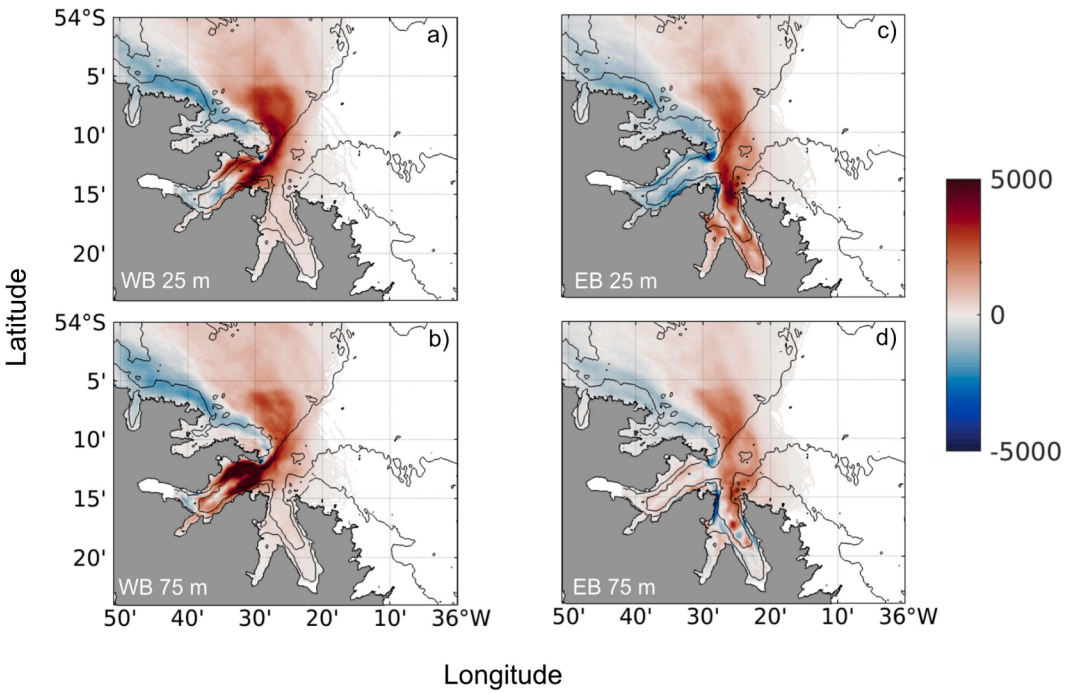

Fig. 17. The difference (test minus BASE) in the number of particles passing through each model grid cell between the BASE run and FÖHN separated into WB (left), EB (right), 25 m releases (above) and 75 m releases (below), as labelled.

in Cumberland West Bay, this circulation shift has likely been happening in recent years, with subglacial discharge potentially now ceased altogether. Nonetheless, this rapid and dramatic change in glacier geometry and subsequent plume dynamics is likely to have a strong influence on the transport and retention of fish larvae, along with other organisms in the bay.

The retreat of Neumayer Glacier since the 1980 s has revealed a shallow inner sill, estimated to be ~ 30 m deep (Zanker et al., 2024). This bathymetric feature may be contributing to the rapid retreat rate due to blocking deep, colder water in the outer basin, and the trapping of warmer waters in the inner basin. The sill may also act as a barrier that helps to retain fish larvae in the inner basin, as found in Atlantic cod populations (Knutsen et al., 2007), and simulated zooplankton in an Arctic fjord (Basedow et al., 2004). In the current oceanographic model configuration, the inner sill is only ~ 2 km from the Neumayer Glacier terminus, as it was in the year 2000. As a result, the sill has little impact on modelled larval retention in the inner basin (not shown) and the changes in plume dynamics with the inner sill are very small during the simulation period. Nevertheless, between the years 2000 to present, it is likely the growing inner basin has become increasingly significant for larval retention, especially if *C. gunnari* are spawning in the inner basin. As a previous study in LeConte Bay, Alaska found, the reflux of freshwater from a glacier due to interacting with a shallow sill can increase flushing time (Hager et al., 2022), so larvae spawned inside the inner basin may have a greater chance of retention, requiring further investigation.

Winds are also expected to (continue to) change in the future, especially the strength of westerly winds (Deng et al., 2022). At South Georgia, this is expected to increase the frequency and intensity of föhn wind events (Bannister and King, 2020). The IBM results find that föhn wind events increase retention in EB, due to the cross-fjord winds modifying the outflow. Though the model atmospheric forcing is coarse and does not include finer-scale interactions with the local orography, the results suggest that föhn winds have the potential to significantly alter the rate of retention year-round through inducing recirculation and eddies, which have previously been identified as mechanisms for retaining zooplankton in an Arctic fjord (Basedow et al., 2004).

4.2.1. *Temperatures*

The results of the IBM modelling highlight the importance of the timing of egg hatching on the retention success of fish larvae due to the seasonal changes in the circulation regime. The drivers of variability in volume transport and therefore larval transport explored in Section 3.1 are interlinked with seasonal temperature changes. Therefore, the timing of hatching affects retention rates through seasonal variability in both temperature and transport. The IBM does not capture, however, the biological implications of timing with respect to the seasonality of ocean temperatures in the fjord. In addition to influencing the timing of spawning and hatching, temperatures influence the size of larvae at hatching, development rate, and length of the larval planktonic phase (Pankhurst and Munday, 2011; Young et al., 2018). With warmer ambient temperatures, the larval pulse in June may have a shorter planktonic phase than the August to October pulse (Cowen and Sponaugle, 2009). Equally, a rise in temperatures for the main hatching period explored in this study may reduce the planktonic phase and increase the chances of retention. This shorter larval phase might be expected if Southern Ocean temperatures significantly warm as predicted by CMIP6 (Climate Model Intercomparison Project 6) experiments (Tonelli et al., 2021).

It is likely that *C. gunnari* at South Georgia are at the upper limit of their thermal tolerance (Kock and Everson, 2003). Living at higher than optimal temperatures requires more energy and increases the likelihood of death on spawning (Kock and Everson, 2003). Therefore, although there may be a higher chance of larval retention, there may also be a higher mortality rate at different life stages, affecting stock size. As the oceans continue to warm due to climate change, this could additionally impact spawning cues, migratory behaviour, and recruitment success (Hill et al., 2005). *C. gunnari* stocks have previously seen a decline due to an increase in the temperature of surface waters following an El Niño-Southern Oscillation in 1998 (Kock and Everson, 2003). There have been smaller temperature changes in deeper waters and an overall trend of increasing temperatures (Whitehouse et al., 2009) that may impact benthic egg development (Pankhurst and Munday, 2011; Young et al., 2018). From 10 years of oceanographic model output (2001 – 2010) the minimum and maximum near-bed temperatures in Cumberland Bay are

−0.7 °C and 2.7 °C, respectively (Zanker et al., 2024). This potential range of 3.4 °C could dramatically alter the egg development and mortality rate depending on the timing of spawning (Young et al., 2018). The near-bed temperatures also differ between WB and EB, where the more prominent outer sill in EB blocks deep, slightly warmer, shelf water entering further in-fjord in winter (Zanker et al. 2024, Figure 5). This difference may give rise to differential egg development and mortality rates between fjord arms. Together with potential changes in circulation, such asymmetry may impact overall larval retention and survival as the climate warms.

4.3. Caveats

4.3.1. Mackerel icefish life history

Relatively little is known about the early life history of *C. gunnari*. The data motivating the experimental design in this study have many limitations such as bias in surveying methods and low temporal and spatial coverage (Fallon et al., 2016). Details of *C. gunnari* spawning phenology, in particular, are unknown. With the recent discovery of a vast icefish (*Neopagetopsis ionah*) breeding colony guarding egg-filled nests (Purser et al., 2022), it is possible that *C. gunnari* exhibits similar behaviours under certain conditions. Multiple-batch spawning as an evolutionary strategy due to short-term fluctuations in environmental conditions is known in other fish species (Folkvord et al., 2016). Bottom trawl survey data from South Georgia reveals high variability in the length frequency dynamics of *C. gunnari* between years. For example, the survey data from the northeast South Georgia shelf from 2004 show high numbers of fish with lengths between 10 and 15 cm, while 2005 finds none in that length range (Fig. S1) (Hollyman, personal communication 2023). The age and length of first spawning is around 2.8 to 3 years at 25 cm (Kock and Everson, 1997). In 2013 and 2021 very few fish were found in this cohort and above (Fig. S1). The interannual variability in cohort frequency may be linked to oceanographic influences on larval retention. Additionally, oceanographic variability may be driving temporary food shortages (in particular Antarctic krill, which relies on transport to the island via the SACCF), which causes a delay in the maturation process and subsequent spawning (Kock and Everson, 2003). All the factors influencing the timing and breeding success of *C. gunnari* could also impact the predator–prey fields. Early spawning and/or hatching due to temperature changes could lead to a mismatch with peak food availability leading to increased mortality through starvation known as the match-mismatch hypothesis (Durant et al., 2007; Hoegh-Guldberg and Bruno, 2010). Overall, stock size fluctuations due to temperature changes are a complex interaction between oceanographic variability, mortality, and prey fields.

Diel vertical migration (DVM) behaviour in *C. gunnari* larvae is another understudied characteristic that may influence retention rates. Vertical migratory behaviour has been observed for late-stage larvae, whereby larvae rise to the near-surface during the day and sink to ~100 m at night, considered reverse DVM (North and Murray, 1992). The reason for this observed behaviour is not well understood, but not assumed to be linked to predator/prey interactions (North and Murray, 1992). In this study, larvae that are released deeper (75 m) in the water column formed a majority of those retained due to avoiding the strong surface outflow. Therefore, introducing vertical migratory behaviour generally would imply a reduction in retention, due to all the larvae now interacting with the surface outflow. Early-stage larvae are less likely to undergo vertical migration for feeding as they are sustained by their yolk sacs, so may remain deeper (Everson, 2003). Later stage larvae may undergo (reverse) DVM but also have the ability to swim against the current to some extent, which could prevent them being flushed out of the bay.

4.3.2. Hydrodynamic model

The underlying hydrodynamic model which produced the flow fields to drive the IBM also has some caveats. The parameterisation of the subglacial plume-driven circulation is not coupled to the ocean model, and the ocean model does not capture the deep inflow driven by entrainment into the plume. This is not expected to impact greatly on the results from the IBM as the larvae are restricted to the upper 100 m and the entrainment generates inflow at depth due to fresh, cold subglacial discharge emerging at the grounding line (Mortensen et al., 2011). The climatological cycle of meltwater runoff is more likely to impact the results. In reality, the meltwater cycle will have interannual variability due to atmospheric warming melting the glaciers, varying both the volume and timing of subglacial discharge. The IBM results are sensitive to the volume and timing of meltwater runoff, and therefore some of the interannual variability in larval retention may be masked by using this climatology. The influence of ice mélange, in particular the melting of large floating icebergs has not been investigated, which may alter stratification and near-surface flows. Nevertheless, the fjord model is of sufficiently high resolution to capture complex cross-fjord flow patterns driven primarily by winds and freshwater runoff and highlights the importance of fine-scale circulation in influencing larval transport and retention. The model may be further improved by the development of higher resolution atmospheric forcing, which would better resolve topographic influences and improve representation of the impact of small-scale atmospheric features on the predicted oceanography of Cumberland Bay and the wider shelf (Hosking et al., 2015).

5. Summary and conclusions

This study utilised a 3D hydrodynamic model of Cumberland Bay, a sub-Antarctic island fjord, to investigate the drivers of oceanographic variability and the influence of such variability on the larval transport of the ecologically and commercially important *C. gunnari*. A series of process tests found the dominant drivers of variability to be seasonal. In summer and autumn, there is an interplay between the warming of the surface waters by the atmospheric forcing and cooling by the freshwater forcing via subglacial discharge. In the winter and spring, freshwater forcing is less dominant, and the interplay is between the atmospheric and boundary forcing. At depth, the boundary forcing drives dense coastal inflow throughout the year and complex intermediary mid-depth exchange, which is modified by the winds. The freshwater forcing gives rise to buoyancy-driven outflow which drives a thick surface outflow in West Bay (WB), while East Bay (EB) has a consistently thin, surface buoyancy-driven outflow, similar to estuarine circulation. The cross-fjord structure of outflow is largely driven by the winds and interactions with the dominant northwestward shelf flows. Experiments with a representation of föhn wind events revealed how the high wind speeds and air temperatures associated with these events can change the sea surface temperature and alter near-surface circulation differentially between the fjord arms, due to their orientation with respect to the wind direction.

The use of an individual-based model (IBM) with particles parameterised to represent *C. gunnari* larvae revealed notable interannual variability in larval retention due to oceanographic variability. Geographical location of hatching is found to be significant as most of the particles successfully retained over the five years started and ended in WB. Linking to the results of the process tests revealed how changes in the timing of the release of the particles in relation to the meltwater forcing cycle would likely impact retention. The results highlighted how the complex and interlinked drivers of variability can influence the oceanography on short time scales and impact retention in not easily predictable ways.

Climate change is likely to have been increasing the frequency and intensity of föhn wind events and altering the volume of glacial meltwater runoff. The sensitivity of retention to föhn winds has been tested, highlighting again that short-term changes in wind speed and direction can alter circulation patterns significantly and impact successful retention, with retention in EB notably increased. Variability in retention due to changes in the volume of meltwater linked to glacier dynamics

responding to climate change has been investigated, finding that the influence of the volume of meltwater depended both on the timing and location of hatching. Most notably, a reduction in the volume of meltwater and therefore subglacial discharge led to an increase in retention in WB for particles released in September and October.

This study has highlighted the importance of oceanographic variability for ecological processes in fjords. Circulation in fjords globally is likely to be impacted by physical processes linked to climate change, with potentially drastic implications for local ecosystems and commercial fisheries. The South Georgia and South Sandwich Islands MPA has become a model for how conservation of marine biodiversity can be achieved through regulating sustainable fisheries (Ocean: Earth's Last Wilderness, Attenborough and Butfield, 2025, Chapter 8). An understanding of the drivers of variability in the fjord circulation regime, and the influence of such variability on ecological processes via modelling and observations, is necessary for adaptive fisheries management and the continued implementation of effective conservation measures.

6. Data statement

The observational data and model output underlying the figures and tables in this paper are available at https://doi.org/10.5281/zenodo.8167711 (Zanker, 2023). The model code for NEMO-4.0.6 is available from the NEMO website (www.nemo-ocean.eu). The HAL software is available at https://github.com/emmafyoung/HAL.

CRediT authorship contribution statement

Joanna Zanker: Writing – review & editing, Writing – original draft, Visualization, Validation, Methodology, Investigation, Formal analysis, Data curation, Conceptualization. **Emma F. Young:** . **Paul Brickle:** Writing – review & editing, Supervision, Funding acquisition, Data curation, Conceptualization. **Ivan Haigh:** Supervision, Project administration.

Declaration of competing interest

The authors declare the following financial interests/personal relationships which may be considered as potential competing interests: Joanna Zanker reports financial support was provided by Polar SeaFish Ltd. If there are other authors, they declare that they have no known competing financial interests or personal relationships that could have appeared to influence the work reported in this paper.

Acknowledgements

This work was supported by the Natural Environment Research Council via the BAS Polar Oceans program and the INSPIRE Doctoral Training Partnership (Grant number: INSPIRE DTP-1). JZ is supported by the UK Research and Innovation (grant no. MR/W011816/1). The authors would like to thank Polar Seafish Ltd for additional support and funding. We thank the Government of South Georgia and the South Sandwich Islands and the crew of the Pharos SG for facilitating and aiding oceanographic data collection. The numerical simulations were carried out on the ARCHER2 UK National Supercomputing Service (https://www.archer2.ac.uk/).

Appendix A. . Description of the meltwater forcing parameterisation following Zanker et al., 2024

As described briefly in the main text (Section 2), for the two large marine-terminating glaciers in Cumberland Bay, the meltwater forcing required consideration of subglacial meltwater plume-driven dynamics. Based on previous knowledge, it is assumed that a majority of surface meltwater from the glaciers descends through crevasses and moulins and enters subglacial channel systems at the bed (Chu 2014). These channels meet the ocean at the grounding line of the marine-terminating glaciers at the fjord head, leading to the rise of subglacial discharge as a buoyant plume (Hewitt, 2020). Thus, the theoretical meltwater cycle is split into 10 % surface runoff and 90 % subglacial discharge. Given the uneven bathymetry, for the purposes of this study, it was assumed that "localized channels" are formed, which emerge at the deepest part of the glacier termini and are a width of one grid cell (~200 m) (Slater et al., 2015). In reality, buoyant plumes tend to rise in contact with the submarine ice face, causing melt and continue to entrain ambient ocean water until they reach neutral buoyancy (or the surface), where they intrude horizontally into the ocean (Hewitt, 2020; Sciascia et al., 2013). A parameterisation is required to represent this in the model due to NEMO4 using the hydrostatic assumption.

The default option for meltwater runoff in NEMO4 is to introduce fresh, cold meltwater into the surface layers of the model, down to a specified depth range. However, this does not capture potentially important increased buoyancy-driven outflow and upwelling of deep waters because of subglacial discharge and could result in unrealistic ocean stratification (Cottier et al., 2010). A new improvement has been developed for this study that adapts the meltwater input by representing the subglacial-discharge plume characteristics according to an offline plume model. The parameterisation developed here follows a similar framework implemented within MITgcm and ROMS (Cowton et al., 2015; Oliver et al., 2020). NEMO4 does not allow for the removal of water, heat and salt in such a way as MITgcm and ROMS. Therefore, a pragmatic compromise was taken by editing an existing NEMO4 routine and using an offline plume model. This offline model requires ocean conditions, which necessitates an iterative process, as follows.

First, the model is run for 10 years (following a year spin-up) with no terrestrial freshwater forcing. The deepest ocean grid cell column adjacent to the glacier is identified as the point to which the subglacial discharge would be directed via the hydraulic gradient. Next, an offline plume model calculates the properties of the plume based on Slater et al (2017, Equations 4a–4d) and the melt rate of the submarine ice face based on Jenkins (2011 Equations 7–9). Inputs to the plume model are temperature and salinity from the previously identified model grid cell column and the theoretical daily subglacial discharge, Q_S m^3s^{-1}. The model is solved for the temperature (°C), salinity, volume per second (Q_P m^3s^{-1}) and depth (D m) at which the plume reaches neutral buoyancy (termination depth) (Fig. 2 in main text), with plume model constants following Slater et al. (2017). Finally, the meltwater properties are set to the plume T and S and inserted into the relevant NEMO4 grid cell from the surface down to the termination depth, D, if the plume reaches neutral buoyancy below the surface, or down to 10 m if the plume reaches the surface. It is not currently possible to simulate a wholly subsurface plume in NEMO4; however, a subsurface plume is ultimately achieved due to the higher density of plume water input compared to the near-surface ocean waters. The surface freshwater runoff (the remaining 10 % of the theoretical daily meltwater) is inserted into an adjacent grid cell to that used for the plume model to simulate the portion that would remain on the glacier's surface running off from supraglacial streams.

The new meltwater parameterization provides a representation of glacier plume and buoyancy-driven outflow within the limitations of the NEMO4 framework, which is not captured by adding fresh, cold meltwater into the surface alone. The caveats of this approach are discussed in previous work (Zanker et al., 2024).

Appendix B. Supplementary data

Supplementary data to this article can be found online at https://doi.org/10.1016/j.pocean.2025.103601.

Data availability

Links to data repositories are available in the 'Data statement' sec-

tion of the manuscript.

References

Arimitsu, M.L., Piatt, J.F., Mueter, F., 2016. Influence of glacier runoff on ecosystem structure in Gulf of Alaska fjords. Mar. Ecol. Prog. Ser. 560. https://doi.org/10.3354/meps11888.

Arneborg, L., Erlandsson, C.P., Liljebladh, B., Stigebrandt, A., 2004. The rate of inflow and mixing during deep-water renewal in a sill fjord. Limnol. Oceanogr. 49 (3). https://doi.org/10.4319/lo.2004.49.3.0768.

Asplin, L., Salvanes, A.G.V., Kristoffersen, J.B., 1999. Nonlocal wind-driven fjord-coast advection and its potential effect on plankton and fish recruitment. Fish. Oceanogr. 8 (4). https://doi.org/10.1046/j.1365-2419.1999.00109.x.

Attenborough, D., & Butfield, C. (2025). *Ocean: Earth's Last Wilderness*.

Bannister, D., King, J., 2015. Föhn winds on South Georgia and their impact on regional climate. Weather 70 (11). https://doi.org/10.1002/wea.2548.

Bannister, D., King, J.C., 2020. The characteristics and temporal variability of föhn winds at King Edward Point, South Georgia. Int. J. Climatol. 40 (5), 2778–2794. https://doi.org/10.1002/joc.6366.

Barlow, K.E., Boyd, I.L., Croxall, J.P., Reid, K., Staniland, I.J., Brierley, A.S., 2002. Are penguins and seals in competition for Antarctic krill at South Georgia? Mar. Biol. https://doi.org/10.1007/s00227-001-0691-7.

Basedow, S.L., Eiane, K., Tverberg, V., Spindler, M., 2004. Advection of zooplankton in an Arctic fjord (Kongsfjorden, Svalbard). Estuar. Coast. Shelf Sci. 60 (1). https://doi.org/10.1016/j.ecss.2003.12.004.

Belchier, M., Lawson, J., 2013. An analysis of temporal variability in abundance, diversity and growth rates within the coastal ichthyoplankton assemblage of South Georgia (sub-Antarctic). Polar Biol. 36 (7), 969–983. https://doi.org/10.1007/s00300-013-1321-9.

Benn, D.I., Cowton, T., Todd, J., Luckman, A., 2017. Glacier Calving in Greenland. Current Climate Change Reports 3 (4). https://doi.org/10.1007/s40641-017-0070-1.

Bosson, J.B., Huss, M., Cauvy-Fraunié, S., Clément, J.C., Costes, G., Fischer, M., Poulenard, J., Arthaud, F., 2023. Future emergence of new ecosystems caused by glacial retreat. Nature 620 (7974). https://doi.org/10.1038/s41586-023-06302-2.

Calderan, S.V., Dornan, T., Fielding, S., Irvine, R., Jackson, J.A., Leaper, R., Liszka, C.M., Olson, P.A., Collins, M.A., 2023. Observations of southern right whales (Eubalaena australis) surface feeding on krill in austral winter at South Georgia. Mar. Mamm. Sci. 39 (4). https://doi.org/10.1111/mms.13025.

Christoffersen, P., Mugford, R.I., Heywood, K.J., Joughin, I., Dowdeswell, J.A., Syvitski, J.P.M., Luckman, A., Benham, T.J., 2011. Warming of waters in an East Greenland fjord prior to glacier retreat: Mechanisms and connection to large-scale atmospheric conditions. Cryosphere. https://doi.org/10.5194/tc-5-701-2011.

Chu, V.W., 2014. Greenland ice sheet hydrology: a review. Prog. Phys. Geogr. 38 (1). https://doi.org/10.1177/0309133313507075.

Clarke, A., Croxall, J.P., Poncet, S., Martin, A.R., Burton, R., 2012. Important bird areas: South Georgia. British Birds 105 (3).

Combes, V., Matano, R.P., Meredith, M.P., Young, E.F., 2023. Variability of the Shelf Circulation Around South Georgia. Southern Ocean. Journal of Geophysical Research: Oceans 128 (2). https://doi.org/10.1029/2022JC019257.

Cook, A.J., Poncet, S., Cooper, A.P.R., Herbert, D.J., Christie, D., 2010. Glacier retreat on South Georgia and implications for the spread of rats. Antarct. Sci. 22 (3), 255–263. https://doi.org/10.1017/S0954102010000064.

Cottier, F.R., Nilsen, F., Skogseth, R., Tverberg, V., Skardhamar, J., Svendsen, H., 2010. Arctic fjords: a review of the oceanographic environment and dominant physical processes. Geochem. Soc. Spec. Publ. 344 (November), 35–50. https://doi.org/10.1144/SP344.4.

Cowen, R.K., Sponaugle, S., 2009. Larval dispersal and marine population connectivity. Ann. Rev. Mar. Sci. 1 (September 2008), 443–466. https://doi.org/10.1146/annurev.marine.010908.163757.

Cowton, T., Slater, D., Sole, A., Goldberg, D., Nienow, P., 2015. Modeling the impact of glacial runoff on fjord circulation and submarine melt rate using a new subgrid-scale parameterization for glacial plumes. J. Geophys. Res. Oceans 120 (2), 796–812. https://doi.org/10.1002/2014JC010324.

Deng, K., Azorin-Molina, C., Yang, S., Hu, C., Zhang, G., Minola, L., Chen, D., 2022. Changes of Southern Hemisphere westerlies in the future warming climate. Atmos. Res. 270. https://doi.org/10.1016/j.atmosres.2022.106040.

Duhamel, G., 1995. New data on spawning, hatching and growth of Champsocephalus gunnari on the shelf of the Kerguelen Islands. CCAMLR Sci 2, 21–34.

Durant, J.M., Hjermann, D., Ottersen, G., Stenseth, N.C., 2007. Climate and the match or mismatch between predator requirements and resource availability. Climate Res. 33 (3). https://doi.org/10.3354/cr033271.

Egbert, G.D., Erofeeva, S.Y., 2002. Efficient inverse modeling of barotropic ocean tides. J. Atmos. Oceanic Tech. 19 (2). https://doi.org/10.1175/1520-0426(2002)019<0183:EIMOBO >2.0.CO;2.

Everson, I., 1992. Managing Southern Ocean krill and fish stocks in a changing environment. Philosoph. Trans. - Royal Soc. London, B 338 (1285). https://doi.org/10.1098/rstb.1992.0151.

Everson, I., 2003. *Original: English Agenda CEMP Review (WG-EMM Agenda Number 2) Agenda Item No(s): Title SPECIES PROFILE: MACKEREL ICEFISH.*

Everson, I., North, A.W., Paul, A., Cooper, R., McWilliam, N.C., Kock, K.H., 2001. Spawning locations of mackerel icefish at South Georgia. CCAMLR Science.

Fallon, N.G., Collins, M.A., Marshall, C.T., Fernandes, P.G., 2016. Assessing consistency of fish survey data: uncertainties in the estimation of mackerel icefish (Champsocephalus gunnari) abundance at South Georgia. Polar Biol. 39 (4). https://doi.org/10.1007/s00300-015-1810-0.

Farías-Barahona, D., Sommer, C., Sauter, T., Bannister, D., Seehaus, T.C., Malz, P., Casassa, G., Mayewski, P.A., Turton, J.V., Braun, M.H., 2020. Detailed quantification of glacier elevation and mass changes in South Georgia. Environ. Res. Lett. 15 (3). https://doi.org/10.1088/1748-9326/ab6b32.

Farmer, D.M., Freeland, H.J., 1983. The physical oceanography of Fjords. Prog. Oceanogr. 12 (2). https://doi.org/10.1016/0079-6611(83)90004-6.

Fogarty, M.J., 2014. The art of ecosystem-based fishery management. Can. J. Fish. Aquat. Sci. 71 (3). https://doi.org/10.1139/cjfas-2013-0203.

Folkvord, A., Gundersen, G., Albretsen, J., Asplin, L., Kaartvedt, S., Giske, J., 2016. Impact of hatch date on early life growth and survival of Mueller's pearlside (Maurolicus muelleri) larvae and life-history consequences. Can. J. Fish. Aquat. Sci. 73 (2). https://doi.org/10.1139/cjfas-2015-0040.

Frolkina, G., Konstantinova, M.P., Trunov, I., 1998. Composition and Characteristics of Ichthyofauna. CCAMLR Sci. 5, 125–164.

Frolkina, Z.A., 2002. Distribution of mackerel icefish (champsocephalus gunnari) (channichthyidae) around South Georgia at various stages of its life cycle. CCAMLR Sci. 9.

Gnanadesikan, A., Slater, R.D., Gruber, N., Sarmiento, J.L., 2001. Oceanic vertical exchange and new production: a comparison between models and observations. Deep-Sea Res. Part II: Topical Studies Oceanograph. 49 (1–3). https://doi.org/10.1016/S0967-0645(01)00107-2.

Griffith, T.W., Anderson, J.B., 1989. Climatic control of sedimentation in bays and fjords of the northern Antarctic Peninsula. Mar. Geol. 85 (2–4). https://doi.org/10.1016/0025-3227(89)90153-9.

Hager, A.O., Sutherland, D.A., Amundson, J.M., Jackson, R.H., Kienholz, C., Motyka, R. J., Nash, J.D., 2022. Subglacial Discharge Reflux and Buoyancy Forcing Drive Seasonality in a Silled Glacial Fjord. J. Geophys. Res. Oceans 127 (5). https://doi.org/10.1029/2021JC018355.

Hersbach, H., Bell, B., Berrisford, P., Hirahara, S., Horányi, A., Muñoz-Sabater, J., Nicolas, J., Peubey, C., Radu, R., Schepers, D., Simmons, A., Soci, C., Abdalla, S., Abellan, X., Balsamo, G., Bechtold, P., Biavati, G., Bidlot, J., Bonavita, M., Thépaut, J.N., 2020. The ERA5 global reanalysis. Q. J. R. Meteorolog. Soc. 146 (730). https://doi.org/10.1002/qj.3803.

Hewitt, I.J., 2020. Subglacial Plumes. Annu. Rev. Fluid Mech. 52 (1), 145–169. https://doi.org/10.1146/annurev-fluid-010719-060252.

Hill, S.L., Reid, K., North, A.W., 2005. Recruitment of mackerel icefish (Champsocephalus gunnari) at South Georgia indicated by predator diets and its relationship with sea surface temperature. Can. J. Fish. Aquat. Sci. https://doi.org/10.1139/f05-157.

Hinrichsen, H.H., Dickey-Collas, M., Huret, M., Peck, M.A., Vikebø, F.B., 2011. Evaluating the suitability of coupled biophysical models for fishery management. ICES J. Mar. Sci. 68 (7). https://doi.org/10.1093/icesjms/fsr056.

Hoegh-Guldberg, O., Bruno, J.F., 2010. The impact of climate change on the world's marine ecosystems. Science 328 (5985). https://doi.org/10.1126/science.1189930.

Hogg, O.T., Huvenne, V.A.I., Griffiths, H.J., Dorschel, B., Linse, K., 2016. Landscape mapping at sub-Antarctic South Georgia provides a protocol for underpinning large-scale marine protected areas. Sci. Rep. 6. https://doi.org/10.1038/srep33163.

Hosking, J.S., Bannister, D., Orr, A., King, J., Young, E., Phillips, T., 2015. Orographic disturbances of surface winds over the shelf waters adjacent to South Georgia. Atmos. Sci. Lett. 16 (1). https://doi.org/10.1002/asl2.519.

Howell, D., Schueller, A.M., Bentley, J.W., Buchheister, A., Chagaris, D., Cieri, M., Drew, K., Lundy, M.G., Pedreschi, D., Reid, D.G., Townsend, H., 2021. Combining ecosystem and single-species modeling to provide ecosystem-based fisheries management advice within current management systems. Front. Mar. Sci. 7. https://doi.org/10.3389/fmars.2020.607831.

Hsieh, C.H., Kim, H.J., Watson, W., Di Lorenzo, E., Sugihara, G., 2009. Climate-driven changes in abundance and distribution of larvae of oceanic fishes in the southern California region. Glob. Chang. Biol. 15 (9). https://doi.org/10.1111/j.1365-2486.2009.01875.x.

Inall, M.E., Gillibrand, P.A., 2010. The physics of mid-latitude fjords: a review. Geochem. Soc. Spec. Publ. 344, 17–33. https://doi.org/10.1144/SP344.3.

Jackson, R.H., Lentz, S.J., Straneo, F., 2018. The dynamics of shelf forcing in Greenlandic fjords. J. Phys. Oceanogr. 48 (11). https://doi.org/10.1175/JPO-D-18-0057.1.

Jenkins, A., 2011. Convection-driven melting near the grounding lines of ice shelves and tidewater glaciers. J. Phys. Oceanogr. https://doi.org/10.1175/JPO-D-11-03.1.

Knutsen, H., Moland Olsen, E., Ciannelli, L., Espeland, S.H., Knutsen, J.A., Simonsen, J. H., Skreslet, S., Stenseth, N.C., 2007. Egg distribution, bottom topography and small-scale cod population structure in a coastal marine system. Mar. Ecol. Prog. Ser. 333, 249–255. https://doi.org/10.3354/meps333249.

Kock, K.H., 1989. Reproduction of the mackerel icefish (Champsocephalus gunnari) and its implications for fisheries management in the Atlantic sector of the Southern Ocean. Select Sci. Pap.

Kock, K.H., Everson, I., 1997. Biology and ecology of mackerel icefish, Champsocephalus gunnari: an Antarctic fish lacking hemoglobin. Comparat. Biochem. Physiol. - A Physiol. https://doi.org/10.1016/S0300-9629(97)86795-3.

Kock, K.H., Everson, I., 2003. Shedding new light on the life cycle of mackerel icefish in the Southern Ocean. J. Fish Biol. 63 (1), 1–21. https://doi.org/10.1046/j.1095-8649.2003.00150.x.

Kowalik Z. Murty, T.S., 1993. Numerical Modelling of Ocean Dynamics. World Scientific.

Landaeta, M.F., López, G., Suárez-Donoso, N., Bustos, C.A., Balbontín, F., 2012. Larval fish distribution, growth and feeding in Patagonian fjords: potential effects of freshwater discharge. Environ. Biol. Fishes 93 (1), 73–87. https://doi.org/10.1007/s10641-011-9891-2.

Lett, C., Ayata, S.D., Huret, M., Irisson, J.O., 2010. Biophysical modelling to investigate the effects of climate change on marine population dispersal and connectivity. Prog. Oceanogr. 87 (1–4). https://doi.org/10.1016/j.pocean.2010.09.005.

Lundesgaard, Ø., Powell, B., Merrifield, M., Hahn-Woernle, L., Winsor, P., 2019. Response of an antarctic Peninsula fjord to summer Katabatic wind events. J. Phys. Oceanogr. https://doi.org/10.1175/JPO-D-18-0119.1.

Madec, G., the NEMO Team, 2019. NEMO ocean engine. Note Du Pôle De Modélisation 27.

Main, C.E., Collins, M.A., Mitchell, R., Belchier, M., 2009. Identifying patterns in the diet of mackerel icefish (Champsocephalus gunnari) at South Georgia using bootstrapped confidence intervals of a dietary index. Polar Biol. 32 (4), 569–581. https://doi.org/10.1007/s00300-008-0552-7.

Meerhoff, E., Tapia, F.J., Sobarzo, M., Castro, L., 2014. Influence of estuarine and secondary circulation on crustacean larval fluxes: a case study from a Patagonian fjord. J. Plankton Res. 37 (1), 168–182. https://doi.org/10.1093/plankt/fbu106.

Mortensen, J., Bendtsen, J., Lennert, K., Rysgaard, S., 2014. Seasonal variability of the circulation system in a west Greenland tidewater outlet glacier fjord, Godthåbsfjord (64°N). J. Geophys. Res. Earth 119 (12). https://doi.org/10.1002/2014JF003267.

Mortensen, J., Lennert, K., Bendtsen, J., Rysgaard, S., 2011. Heat sources for glacial melt in a sub-Arctic fjord (Godthåbsfjord) in contact with the Greenland Ice Sheet. J. Geophys. Res. Oceans 116 (1), 1–13. https://doi.org/10.1029/2010JC006528.

Myksvoll, M.S., 2012. *Connectivity among subpopulations of Norwegian Coastal cod Impacts of physical-biological factors during egg stages*.

Myksvoll, M.S., Sundby, S., Ådlandsvik, B., Vikebø, F.B., 2011. Retention of coastal cod eggs in a fjord caused by interactions between egg buoyancy and circulation pattern. Mar. Coastal Fish. 3 (1). https://doi.org/10.1080/19425120.2011.595258.

North, A.W., 2001. Early life history strategies of notothenioids at South Georgia. J. Fish Biol. 58 (2), 496–505. https://doi.org/10.1006/jfbi.2000.1469.

North, A.W., Murray, A.W.A., 1992. Abundance and diurnal vertical distribution of fish larvae in early spring and summer in a fjord at South Georgia. Antarct. Sci. https://doi.org/10.1017/S0954102092000609.

Okubo, A., 1971. Oceanic diffusion diagrams. Deep-Sea Res. Oceanogr. Abstr. 18 (8), 789–802. https://doi.org/10.1016/0011-7471(71)90046-5.

Oliver, H., Castelao, R.M., Wang, C., Yager, P.L., 2020. Meltwater-Enhanced Nutrient Export from Greenland's Glacial Fjords: a Sensitivity Analysis. J. Geophys. Res. Oceans 125 (7). https://doi.org/10.1029/2020JC016185.

Pankhurst, N.W., Munday, P.L., 2011. Effects of climate change on fish reproduction and early life history stages. Mar. Freshw. Res. 62 (9). https://doi.org/10.1071/MF10269.

Parkes, G.B., Americas, M.R.A.G., 2000. Protecting young fish and spawning aggregations of Cilampsocephalus Guwari in Subarea 48.3 (South Georgia): a review. CCAMLR Sci. 7, 75–86.

Purser, A., Hehemann, L., Boehringer, L., Tippenhauer, S., Wege, M., Bornemann, H., Pineda-Metz, S.E.A., Flintrop, C.M., Koch, F., Hellmer, H.H., Burkhardt-Holm, P., Janout, M., Werner, E., Glemser, B., Balaguer, J., Rogge, A., Holtappels, M., Wenzhoefer, F., 2022. A vast icefish breeding colony discovered in the Antarctic. Curr. Biol. 32 (4). https://doi.org/10.1016/j.cub.2021.12.022.

Robinson, J., Popova, E.E., Srokosz, M.A., Yool, A., 2016. A tale of three islands: Downstream natural iron fertilization in the Southern Ocean. J. Geophys. Res. Oceans. https://doi.org/10.1002/2015JC011319.

Rounce, D.R., Hock, R., Maussion, F., Hugonnet, R., Kochtitzky, W., Huss, M., Berthier, E., Brinkerhoff, D., Compagno, L., Copland, L., Farinotti, D., Menounos, B., McNabb, R.W., 2023. Global glacier change in the 21st century: every increase in temperature matters. Science 379 (6627). https://doi.org/10.1126/science.abo1324.

Sciascia, R., Straneo, F., Cenedese, C., Heimbach, P., 2013. Seasonal variability of submarine melt rate and circulation in an East Greenland fjord. J. Geophys. Res. Oceans 118 (May), 2492–2506. https://doi.org/10.1002/jgrc.20142.

Skarðhamar, J., Svendsen, H., 2010. *Short-term hydrographic variability in a stratified Arctic fjord. 2*, 51–60.

Slater, D.A., Nienow, P.W., Cowton, T.R., Goldberg, D.N., Sole, A.J., 2015. Effect of near-terminus subglacial hydrology on tidewater glacier submarine melt rates. Geophys. Res. Lett. 42 (8). https://doi.org/10.1002/2014GL062494.

Slater, D.A., Nienow, P.W., Goldberg, D.N., Cowton, T.R., Sole, A.J., 2017. A model for tidewater glacier undercutting by submarine melting. Geophys. Res. Lett. https://doi.org/10.1002/2016GL072374.

Slater, D.A., Straneo, F., 2022. Submarine melting of glaciers in Greenland amplified by atmospheric warming. Nat. Geosci. 15 (10). https://doi.org/10.1038/s41561-022-01035-9.

Spall, M.A., Jackson, R.H., Straneo, F., 2017. Katabatic Wind-Driven Exchange in Fjords. J. Geophys. Res. Oceans 122 (10). https://doi.org/10.1002/2017JC013026.

Straneo, F., Cenedese, C., 2015. The dynamics of greenland's glacial fjords and their role in climate. Ann. Rev. Mar. Sci. 7. https://doi.org/10.1146/annurev-marine-010213-135133.

Straneo, F., Hamilton, G.S., Sutherland, D.A., Stearns, L.A., Davidson, F., Hammill, M.O., Stenson, G.B., Rosing-asvid, A., 2010. Rapid circulation of warm subtropical waters in a major glacial fjord in East Greenland. Nat. Geosci. 3 (February). https://doi.org/10.1038/ngeo764.

Synnes, A.E.W., Huserbråten, M., Knutsen, H., Jorde, P.E., Sodeland, M., Moland, E., 2021. Local recruitment of Atlantic cod and putative source spawning areas in a coastal seascape. ICES J. Mar. Sci. 78 (10). https://doi.org/10.1093/icesjms/fsab226.

Talley, L.D., Pickard, G.L., Emery, W.J., Swift, J.H., 2011. Chapter S8 - Gravity Waves, Tides, and Coastal Oceanography: Supplementary Materials BT - Descriptive Physical Oceanography (Sixth Edition). In *Descriptive Physical Oceanography Sixth Edition*.

Thomas, Z., Turney, C., Allan, R., Colwell, S., Kelly, G., Lister, D., Jones, P., Beswick, M., Alexander, L., Lippmann, T., Herold, N., Jones, R., 2018. A new daily observational record from Grytviken, South Georgia: Exploring twentieth-century extremes in the South Atlantic. J. Clim. 31 (5), 1743–1755. https://doi.org/10.1175/JCLI-D-17-0353.1.

Tonelli, M., Signori, C.N., Bendia, A., Neiva, J., Ferrero, B., Pellizari, V., Wainer, I., 2021. Climate Projections for the Southern Ocean Reveal Impacts in the Marine Microbial Communities following increases in Sea Surface Temperature. Front. Mar. Sci. 8. https://doi.org/10.3389/fmars.2021.636226.

Trathan, P.N., Brierley, A.S., Brandon, M.A., Bone, D.G., Goss, C., Grant, S.A., Murphy, E. J., Watkins, J.L., 2003. Oceanographic variability and changes in Antarctic krill (Euphausia superba) abundance at South Georgia. Fish. Oceanogr. 12 (6). https://doi.org/10.1046/j.1365-2419.2003.00268.x.

Trathan, P.N., Collins, M.A., Grant, S.M., Belchier, M., Barnes, D.K.A., Brown, J., Staniland, I.J., 2014. The South Georgia and the South Sandwich Islands MPA. Adv. Mar. Biol. https://doi.org/10.1016/b978-0-12-800214-8.00002-5.

Ward, P., 1989. The distribution of zooplankton in an Antarctic fjord at South Georgia during summer and winter. Antarct. Sci. 1 (2). https://doi.org/10.1017/S0954102089000210.

Wesławski, J.M., Kendall, M.A., Włodarska-Kowalczuk, M., Iken, K., Kedra, M., Legezynska, J., Sejr, M.K., 2011. Climate change effects on Arctic fjord and coastal macrobenthic diversity-observations and predictions. In. Mar. Biodivers. Vol. 41, Issue 1. https://doi.org/10.1007/s12526-010-0073-9.

Węsławski, J.M., Pedersen, G., Petersen, S.F., Poraziński, K., 2000. Entrapment of macroplankton in an Arctic fjord basin, Kongsfjorden, Svalbard. Oceanologia 42 (1), 57–69.

Whitehouse, M.J., Atkinson, A., Ward, P., Korb, R.E., Rothery, P., Fielding, S., 2009. Role of krill versus bottom-up factors in controlling phytoplankton biomass in the northern Antarctic waters of South Georgia. Mar. Ecol. Prog. Ser. 393. https://doi.org/10.3354/meps08288.

Young, E., M.E., T. P., 2016. *High-resolution ocean modelling of the South Georgia and South Orkney Islands region*.

Young, E.F., 2024. *HAL: Vol. v1.0*. Zenodo.

Young, E.F., Meredith, M.P., Murphy, E.J., Carvalho, G.R., 2011. High-resolution modelling of the shelf and open ocean adjacent to South Georgia, Southern Ocean. Deep-Sea Res. Part II: Topical Studies Oceanograph. 58 (13–16). https://doi.org/10.1016/j.dsr2.2009.11.003.

Young, E.F., Rock, J., Meredith, M.P., Belchier, M., Murphy, E.J., Carvalho, G.R., 2012. Physical and behavioural influences on larval fish retention: Contrasting patterns in two Antarctic fishes. Mar. Ecol. Prog. Ser. 465, 201–215. https://doi.org/10.3354/meps09908.

Young, E.F., Thorpe, S.E., Banglawala, N., Murphy, E.J., 2014. Variability in transport pathways on and around the South Georgia shelf, Southern Ocean: Implications for recruitment and retention. J. Geophys. Res. Oceans 119 (1), 241–252. https://doi.org/10.1002/2013JC009348.

Young, E.F., Tysklind, N., Meredith, M.P., de Bruyn, M., Belchier, M., Murphy, E.J., Carvalho, G.R., 2018. Stepping stones to isolation: Impacts of a changing climate on the connectivity of fragmented fish populations. Evol. Appl. 11 (6). https://doi.org/10.1111/eva.12613.

Zanker, J.C., Young, E., Holland, P.R., Haigh, I.D., Brickle, P., 2024. Oceanographic Variability in Cumberland Bay, South Georgia, and its Implications for Glacier Retreat. J. Geophys. Res. Oceans 129 (2). https://doi.org/10.1029/2023JC020507.

Zemp, M., Huss, M., Thibert, E., Eckert, N., McNabb, R., Huber, J., Barandun, M., Machguth, H., Nussbaumer, S.U., Gärtner-Roer, I., Thomson, L., Paul, F., Maussion, F., Kutuzov, S., Cogley, J.G., 2019. Global glacier mass changes and their contributions to sea-level rise. Nature 568 (7752). https://doi.org/10.1038/s41586-019-1071-0 from 1961 to 2016.

Ziegler, A.F., Hahn-Woernle, L., Powell, B., Smith, C.R., 2020. Larval dispersal modeling suggests limited ecological connectivity between fjords on the West Antarctic peninsula. Integr. Comp. Biol. 60 (6), 1369–1385. https://doi.org/10.1093/icb/icaa094.